TIME-VARYING CONCENTRATION-DEPENDENT INTERDIFFUSION COEFFICIENT IN THE Cu-Ni SYSTEM

By

Tian Guan

A Thesis Submitted to the Faculty of Graduate Studies, University of Manitoba

in Partial Fulfillment of The Requirement for The Degree of

MASTER OF SCIENCE

Department of Mechanical Engineering

University of Manitoba

Winnipeg

Abstract

Solid-state diffusion has attracted substantial research attention due to its key role in metallic materials processing and performance analysis. The isothermal interdiffusion coefficient is one of the crucial parameters for characterizing this process. Although the interdiffusion coefficient is commonly acknowledged as a function of temperature and concentration ($D = F(C, T)$), its time dependence cannot be neglected due to the possible effect of diffusion-induced stress (**DIS**).

The aim in the present work is to experimentally verify the occurrence of time effect on the interdiffusion coefficient in a copper-nickel (Cu-Ni) system and then study its most suggestive underlying factor. To avoid the non-trivial errors that arise from the assumption that the initial concentration profile is a "step-function" in space, a new method that utilizes two concentration profiles is used in this work to calculate the concentration-dependent interdiffusion coefficients.

The results verify that, in contrast to what is commonly recognized, the interdiffusion coefficient is not only a function of temperature and concentration but can also significantly vary with diffusion time due to the presence of **DIS**. This can considerably affect the accuracy of theoretical analysis and predictions of the diffusion process in practical applications such as welding, coating, and heat treatments.

Acknowledgements

I would like to thank Dr. Olanrewaju A. Ojo for offering me this meaningful research opportunity and for all the valuable guidance and profound advice. Additionally, I want to thank Dr. Lina Zhang for providing lab training and equipment maintenance. Finally, I also want to express my gratitude to my parents in China and my friends at the University of Manitoba for their support.

The days during the COVID-19 pandemic have been challenging and significantly impacted the entire experimental schedule. Fortunately, with the support from Dr. Olanrewaju A. Ojo, Dr. Oluwadara Afolabi, Dr. Osamudiamen Olaye, Mr. Maciel Herter (M.Sc.), Mike Boskwick (lab technician) and Dan Rossong (workshop technician), I was able to complete my research work on time. I am thankful that we could encourage one another and get through it. I wish the best to you all and hope everything can get back on track soon.

Table of Contents

List of Tables

List of Figures

List of Abbreviations

BM – Boltzmann-Matano

CALPHAD – Calculation of phase diagrams

DICTRA – Diffusion-controlled transformations

DIS – Diffusion-induced stress

EDM – Electrical discharge machining

EDS – Energy dispersive (x-ray) spectrometer

FSA – Forward simulation analysis

GBD – Grain boundary diffusion

OM – Optical microscope

PCHIP – Piecewise cubic Hermite interpolating polynomial

SEM – Scanning electron microscope

SF – Sauer-Freise

SMA – Simple moving average

List of Symbols

C – Concentration (at%)

$\widetilde{D}(C)$ – Concentration-dependent interdiffusion coefficient or interdiffusion coefficient curve plotted against concentration (m^2/s)

D_{Ave} – Average interdiffusion coefficient (m^2/s)

T – Diffusion treatment temperature (°C)

t – Diffusion treatment time (hour)

$\frac{\partial C}{\partial X}$ – Concentration gradient in space

J_i – Flux of component i

ft – Foot/feet (length unit)

lb – Pound(s) (force unit)

N – Newton (force unit)

K – Kelvin (temperature unit)

°C – Celsius (temperature unit)

mA – Milliampere (current unit)

μm – Micrometer(s) (length unit)

mm – Millimeter(s) (length unit)

cm – Centimeter(s) (length unit)

m – Meter(s) (length unit)

s – Second(s) (time unit)

h – Hour(s) (time unit)

mol(s) – Mole, amount of substance, 6.02×10^{23}

Al – Aluminum (solid state)

Ar – Argon (gas state)

Co – Cobalt (solid state)

Cu – Copper (solid state)

$Cu_{90}Ni_{10}$ – Copper-based alloy containing 90 at% of copper and 10 at% of nickel (solid state)

Fe – Iron (solid state)

H_2BO_3 – Boric acid

HCl – Hydrochloric acid

H_2SO_4 – Sulfuric acid

NaOH – Sodium hydroxide

Na_2CO_3 – Sodium carbonate

Na_2HPO_4 – Disodium phosphate

Ni – Nickel (solid state)

$NiSO_4 \cdot 6H_2O$ – Nickel sulphate hexahydrate

$NiCl_2 \cdot 6H_2O$ – Nickel chloride hexahydrate

SiC – Silicon carbide (grinding particles on sandpaper)

1. Introduction

1.1. Background

Solid diffusion is a widely applied technique that affects various industrial processes, including sintering, coating, jointing, alloy homogenization, solidification, recrystallization, grain boundary migration, etc. It is a fundamental process with profound significance in the industry.

There are several types of diffusion coefficients for quantifying diffusion processes. The most common ones are intrinsic and impurity diffusion coefficients, and the focus point of this work – interdiffusion coefficients ($\widetilde{D}$). Generally speaking, the interdiffusion coefficient is a function of concentration and temperature ($\boldsymbol{D = F(C, T)}$), and would not change with diffusion time, which means that it is not isothermally time-dependent.

However, there are reported data [1–10] showing that the interdiffusion coefficient could be significantly influenced when the diffusion time changes. This can be described as the time effect on the interdiffusion coefficient. Nevertheless, this concept has not been universally acknowledged, and the focus of most previous studies is not on the time effect.

Furthermore, the underlying factor of this time effect has not been thoroughly investigated. According to published studies [4, 10–28], diffusion-induced stress **(DIS)** is inevitably generated due to imbalanced diffusion fluxes and crystal lattice distortion. Also, the DIS has a strong correlation with interdiffusion fluxes, thus can evolve with changing concentration gradients in space ($\frac{\partial C}{\partial X}$). In addition, the DIS has the ability to influence the interdiffusion coefficient. This is why it is potentially being the most suggestive underlying factor of time effect, and one can verify whether DIS is the underlying factor by using the $\frac{\partial C}{\partial X}$ as the indirect investigation approach.

An investigation of the time effect on interdiffusion coefficients is essential. If the time effect is not considered, the interdiffusion coefficient estimation would not be either accurate or reliable. This is unacceptable due to the strong correlation between diffusion in metals and the properties of metallic materials, which are the fundamental focuses of physical metallurgists.

For example, an application for this time effect in the copper-nickel (Cu-Ni) system is related to the thermal ageing (which can cause a negative influence) of Ni-coated Cu conductors at elevated temperatures. In this case, the interdiffusion coefficient is a crucial parameter for estimating service life and performance since the diffusion between Cu and Ni is one of the primary reasons for thermal ageing at elevated temperatures [29]. Correspondingly, the time effect can significantly influence these estimations, thus making this study necessary.

Moreover, a more precise estimation can benefit alloy design and assessment. For instance, a reliable interdiffusion coefficient database can assist with diffusion-controlled processes and simulation of multi-component alloys [10, 30–34], such as diffusion-controlled transformations (DICTRA) [31, 34] and calculation of phase diagrams (CALPHAD) methods [33, 34].

1.2. Research Motivation

It is conventionally acknowledged that the isothermal concentration-dependent interdiffusion coefficient is not time-dependent [14]. However, studies [1–10] have reported data showing cases that contradict this conventional recognition of time-independent. Therefore, there is a conflict between conventional acknowledgements and reported experimental results found in [1–10], which requires further investigation and verification. Thus, solving this conflict is the motivation for this work.

1.3. Research Objectives

The objective of this work is to experimentally verify the occurrence of the time effect on the isothermal concentration-dependent interdiffusion coefficient in the Cu-Ni system at elevated temperatures. Subsequently, to verify if the time effect is attributable to **DIS** by studying the influence of change in concentration gradient on the interdiffusion coefficient, since the variation in $\frac{\partial C}{\partial X}$ has a strong correlation with **DIS**.

1.4. Work Done and Key Findings

A number of diffusion experiments in the Cu-Ni system have been carried out. Then, metallography samples were prepared for concentration profile measurements of all diffusion couples. A data smoothing technique is implemented in this study to minimize the uncertainty/noise of the raw data. This data smoothing process includes two smoothing algorithms, including piecewise cubic Hermite interpolating polynomial (PCHIP) [35] (built-in function of MATLAB®) and simple moving average (SMA) [32, 36, 37]. MATLAB® code scripts are developed and implemented for data smoothing with SMA and PCHIP algorithms, profile averaging, and interdiffusion coefficients calculation. In addition, the reliability of these code scripts is validated by using a forward simulation analysis (FSA) code script [10, 32].

An overall summary of the experiments and data analysis is provided below.

i. The sample preparation process is developed and implemented.
ii. A series of diffusion treatment experiments for different conditions are conducted.
iii. All of the samples are then visually inspected under an optical microscope (OM) to avoid unintentional contamination or oxidation, especially near the interface of dissimilar metals.

iv. Concentration profiles are measured under a scanning electron microscope (SEM) with an energy dispersive (x-ray) spectrometer (EDS) (voltage: 20 kV).

v. The reliability of the experimental data is validated by repeating some of the diffusion treatments.

vi. All of the raw data are smoothed and analyzed by using the MATLAB® code scripts.

vii. Error bars and *p*-values of the *t-statistics* are determined.

viii. $\widetilde{D}(C)$ curves with error bars are plotted in figures for comparison, and the D_{Ave} results are summarized in tables.

By using the analyzed data with error bars and *p*-values of the *t-statistics*, it is found that in contrast to conventional findings, the concentration-dependent interdiffusion coefficient ($\widetilde{D}(C)$) is **NOT** isothermally constant with diffusion time but time-varying. Moreover, the variation in the concentration gradient ($\frac{\partial C}{\partial X}$) can have a noticeable influence on the $\widetilde{D}(C)$ when diffusion time is kept constant. Since there is a strong correlation between the variations in $\frac{\partial C}{\partial X}$ and DIS, the influence can be attributed to the **DIS**. Thus, one can verify if the DIS is the most suggestive underlying factor of time effect on interdiffusion coefficient in Cu-Ni system at high temperatures.

1.5. Thesis Structure

There are six chapters in this work, as follows:

I. Chapter 1 includes the background, research motivation and research objectives, work done and key findings, and thesis structure.

II. Chapter 2 is the literature review, including:

   i. The theoretical foundations of the diffusion process (Fick's laws of diffusion, etc.)

   ii. Analytical equations for diffusion coefficients which include:

a. Conventional (1-profile) methods with a single concentration profile
b. Recently developed (2-profile) methods with two concentration profiles (e.g., 2-profile BM and 2-profile SF).
c. A straightforward comparison indicator: average interdiffusion coefficient.
d. A forward simulation analysis (FSA) for validating the code scripts.

iii. Time-varying concentration-dependent interdiffusion coefficient including:
a. Reported data from other studies that have informed this work
b. Potential underlying factors of the time effect:
a) Introduction of the types of diffusion in a polycrystalline system
b) Introduction of DIS
c) Changes in interdiffusion driving forces

III. Chapter 3 contains the methods of the diffusion experiments and data analysis, including:
i. Raw materials
ii. Methods of sample preparation
iii. Parameters (diffusion temperature, diffusion time, etc.) of diffusion treatments
iv. Methods of data measurement, smoothing and analysis
v. Reliability checks of measured data

IV. Chapter 4 provides the results and discussion, including:
i. Results that validate the time effect on interdiffusion coefficients
ii. Discussion of the most suggestive underlying factor of time effect
iii. Supporting information for investigating the influence of DIS on interdiffusion

V. Chapter 5 is the summary and conclusion of this work.

VI. Chapter 6 discusses the limitations of this work and recommended future works.

2. Literature Review

2.1. Fick's Laws of Diffusion

The diffusion process is related to many different properties of materials, and an analysis of this process is the primary interest of physical metallurgists. Fick's laws of diffusion describe diffusions which govern this field of study. The laws were derived by a German physician and physiologist, Adolf Fick, in 1855, including the first and second laws, as discussed below.

2.1.1. Fick's First Law

In most conditions, metal atoms flow in the manner of reducing the concentration gradients across a given plane through heat treatment of inhomogeneous single-phase alloys. For instance, in an "infinite" system (the surface concentration remains constant), the $\frac{\partial C}{\partial X}$ is infinitely large at the initial stage, but as the diffusion process continues, the $\frac{\partial C}{\partial X}$ continues to decrease. Eventually, the diffusion couple reaches homogeneity after a significantly prolonged period of heat treatment.

The equation of Fick's first law [14, 39] is shown as follows:

$$J_1 = -D_1 \left[\frac{\partial C_1}{\partial X}\right]_t$$

Equation 2.1

where D_1 is called the diffusion coefficient [m^2/s] of component *1*, C_1 is the concentration of the diffusion component *1*, and *X* is the distance in the direction where the diffusion occurs.

Equation 2.1 accommodates the fact that the flux reduces to zero when the couple becomes homogeneous after a considerably prolonged period of heat treatments.

2.1.2. Fick's Second Law

However, Fick's first law is not convenient when the system is in a non-steady state. Therefore, a second differential equation is essential for such a state. As shown in *Figure 2.1*, the following equation can be derived by considering that the volume of the element is $1 \cdot \Delta x$ (unit area × thickness) and combining it with *Equation 2.1*. The outcome is:

$$J_1 - J_2 = \Delta x \left(\frac{\partial C}{\partial t}\right) = -\Delta x \left(\frac{\partial J}{\partial x}\right)$$

Equation 2.2

Equation 2.3 is Fick's second law of diffusion [14, 39], shown as follows:

$$\frac{\partial C}{\partial t} = \frac{\partial}{\partial x}\left[D \frac{\partial C}{\partial x}\right]$$

Equation 2.3

And if *D* is not a function of the distance in space (*x*), then *Equation 2.3* becomes:

$$\frac{\partial C}{\partial t} = D \frac{\partial^2 C}{\partial x^2}$$

Equation 2.4

However, using a partial differential equation for analytical diffusion analysis is not suitable. Therefore, the well-known Boltzmann's transformation was implemented by introducing the Boltzmann variable ($\varepsilon = \frac{x}{2\sqrt{t}}$) to the derivation, as details will be presented in the next section.

2.1.3. Boltzmann's Transformation and the "Step-function" Assumption

Since differential equations are not suitable for the analytical calculation of interdiffusion coefficients, Boltzmann's transformation becomes essential in filling the gap. The Boltzmann-

Matano (BM) equation is the most common method used, which is derived from a partial differential equation that results from Fick's second law. The BM equation is used to estimate the interdiffusion coefficient of an isothermal binary system.

The Boltzmann's transformation is shown as follows:

$$\frac{\partial C}{\partial t} = \frac{\partial}{\partial x}\left[D\frac{\partial C}{\partial x}\right] \;\&\; \xi = \frac{x}{2\sqrt{t}}$$

Equation 2.5

The partial derivatives of ξ are:

$$\frac{\partial \varepsilon}{\partial t} = -\frac{\varepsilon}{2t} \;\&\; \frac{\partial \varepsilon}{\partial x} = \frac{1}{2\sqrt{t}}$$

Equation 2.6

Therefore, Fick's second law can be rewritten as:

$$-2\varepsilon\frac{dC}{d\varepsilon} = \frac{d}{d\varepsilon}\left[D\frac{dC}{d\varepsilon}\right] \;\&\; \text{Integration Form: } -2\int_{C_R}^{C}\varepsilon\, dC = \int_{C_R}^{C} d\left[D\frac{dC}{d\varepsilon}\right]$$

Equation 2.7

In this way, when considering the diffusion time (t) as a given and constant variable:

$$D(C) = -\frac{1}{2t}\cdot\frac{\int_{C_R}^{C}(x - x_M)\,\mathrm{d}C}{\left(\frac{\mathrm{d}C}{\mathrm{d}x}\right)}$$

Equation 2.8

where C is the concentration, C_R is the concentration of the right end, x is the distance, t is the diffusion treatment time, and x_M is the location of the Matano interface.

This *Equation 2.8* is the conventional 1-profile BM equation for calculating the interdiffusion coefficient, where all of the distance data (x) are realigned with the Matano interface.

However, it is worth noting that the 1-profile BM equation is reliable only if a "step-function" type of initial profile is assumed, which means the initial solute distribution must be uniform on either side of the interface, e.g., having 0 at% Ni or 100 at% Cu on the left side and 100 at% Ni or 0 at% Cu on the right side, as shown in *Figure 2.2*.

Generally speaking, thermal bonding is a necessary step for preparing stress-free diffusion couples in most studies. Therefore, interdiffusion between the dissimilar metals will take place to some extent and result in a non-uniform solute distribution prior to diffusion treatments. As a result, the difference between the assumed "step-function" initial concentration profile and the actual concentration profile becomes the non-trivial error.

In other studies that use 1-profile equations, the diffusion treatments for a prolonged period of time (e.g., 100h, 120h) were performed to minimize this non-trivial error. This is because the plotted difference between "step-function" and "actual profile" (marked with a blue star – "★" in *Figure 2.2*) becomes less noticeable when compared to the concentration profile after an adequate diffusion treatment. In other words, the error is reduced with a longer diffusion treatment time. Once this difference is less than 5% (an empirical benchmark) of the final result, the error becomes negligible. In this case, it is possible to consider that the "actual profile" is equivalent to the "step-function" assumption.

On the contrary, if the diffusion treatment time is too short, the difference (marked with a blue star – "★" in *Figure 2.2*) becomes significant (not negligible), thus resulting in a considerate computational error. Moreover, it is difficult to track the interdiffusion coefficient for a time interval (e.g., 5-25 h and 25-75 h) by using 1-profile equations. Due to these limitations, the 2-profile equations are preferred and will be discussed in the later sections.

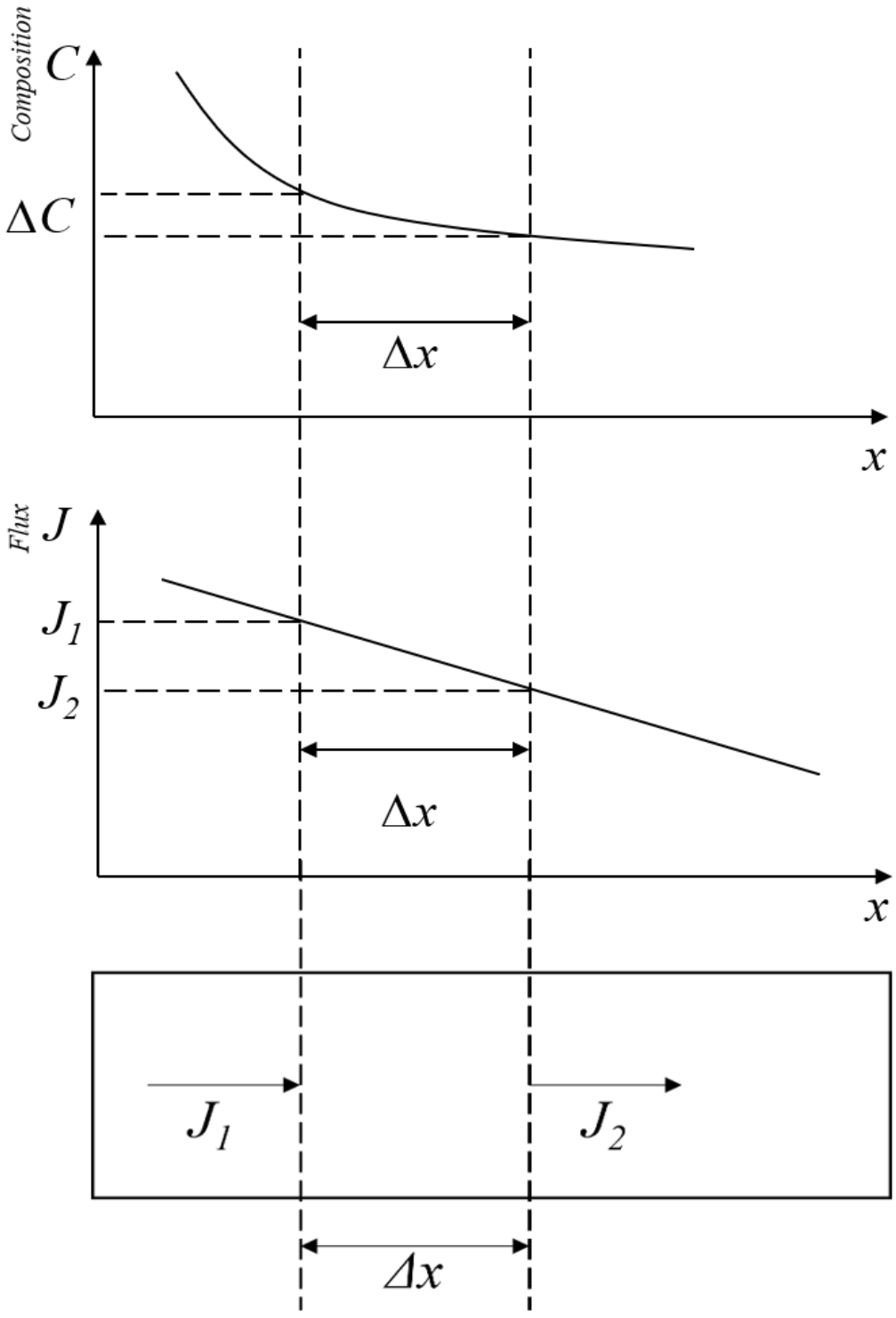

Figure 2.1 – Volume Element for Deriving Fick's Laws

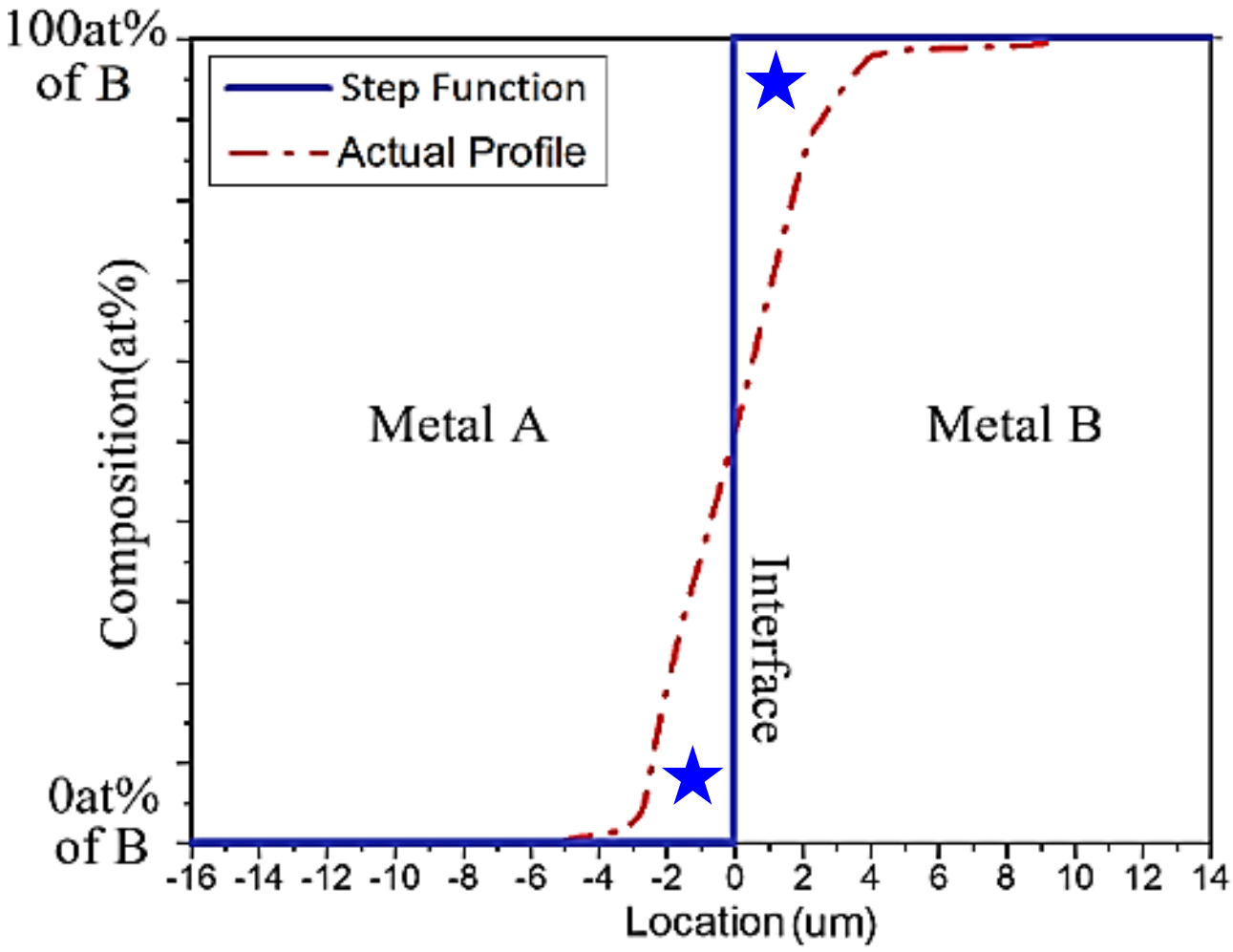

Figure 2.2 – "Step-Function" Assumption and As-bonded Concentration Profile

2.2. Equations for Estimating Interdiffusion Coefficient

2.2.1. Constant Interdiffusion Coefficient

To determine the constant interdiffusion coefficient for a thin-film diffusion couple, the following equation [14, 39] is used:

$$C(x,t) = \frac{bC_0}{2\sqrt{\pi Dt}} exp\left[-\frac{x^2}{4Dt}\right]$$

Equation 2.9

where b is the thickness of the film and C_0 is the solute concentration on the end of a long rod of solute-free material when the diffusion treatment time $t = 0$.

To determine the constant interdiffusion coefficient for a pair of semi-infinite solids, the following equation [14, 39] can be used:

$$C(x,t) = \frac{C'}{2}\left[1 + erf\left(\frac{x}{2\sqrt{Dt}}\right)\right]$$

Equation 2.10

To determine the constant interdiffusion coefficient for the system with constant surface concentration, the following equation [14], [39] can be used:

$$C(x,t) = C'\left[1 - erf\left(\frac{x}{2\sqrt{Dt}}\right)\right]$$

Equation 2.11

where C' is the concentration of the infinite end of the diffusion couple.

2.2.2. 1-profile Concentration-dependent Interdiffusion Coefficient

The BM method requires locating the Matano interface, and the algorithm for determining the location of the Matano interface (x_M) [14, 40] is shown as follows:

$$\int_{\infty}^{x_M} (1 - C)\,\mathrm{d}x = \int_{x_M}^{\infty} C\,\mathrm{d}x$$

Equation 2.12

Since the BM method is a graphical method, its accuracy significantly depends on precisely finding the Matano interface location [2, 14, 38]. Other algorithms that do not require the Matano interface could help to reduce computational workload and accordingly increase computational accuracy. An example is the SF equation which can provide a good estimation of the interdiffusion coefficient without the need to determine x_M:

$$D = -\frac{1}{2t}\left(\frac{\mathrm{d}x}{\mathrm{d}Y}\right)\left[Y\int_{-\infty}^{x}(1 - Y)\,\mathrm{d}x + (1 - Y)\int_{x}^{+\infty} Y\,\mathrm{d}x\right]$$

Equation 2.13

where Y is the molar ratio (relative concentration, from 0.0 to 1.0), and $Y = \frac{C}{C_L - C_R}$.

Computational errors can be somewhat reduced by using SF instead of BM equation because determining of the Matano interface is not required [38, 40]. Therefore, the SF and 2-profile SF equations are preferred in this study.

2.2.3. 2-profile Concentration-dependent Interdiffusion Coefficient

As previously stated, the time of diffusion treatment in previous studies tends to be longer to reduce the computational error. On the other hand, there is a large margin of error when reducing the

diffusion time. In this case, the conventional single profile (1-profile) methods cannot accurately estimate the interdiffusion coefficients of short-time diffusion or diffusion within a specific time interval (e.g., 5-25 h and 25-75 h). Therefore, an analytical method [38] without the "step-function" assumption is required, as presented in the following sections.

2.2.3.1. 2-profile Boltzmann-Matano Equation

The theoretical foundation of the 2-profile equations is still Fick's second law, as indicated in Olaye and Ojo [38], and the derivation is shown as follows. The segmentation (shown in [38]) is along the concentration axis in a plotted concentration profile:

$$\mathrm{d}A = \left(x_f - x_i\right)\mathrm{d}C$$

Equation 2.14

where *dA* is the segmentation area, x_f and x_i represent the distance for a final and initial profile at a selected concentration point respectively, and the *dC* is the segmentation of the concentration. The concentration can be defined as the amount of solute (m_i) per unit volume (*V*). The volume of each segmentation is defined as the section area (A_s) by distance differential ($x_f - x_i$).

Thus, *Equation 2.14* can be further derived into *Equation 2.15* [38]:

$$\mathrm{d}A = \left(x_f - x_i\right)\mathrm{d}C \;=\; \frac{\left(x_f - x_i\right)\mathrm{d}m}{A_s\left(x_f - x_i\right)} = \frac{\mathrm{d}m}{A_s}$$

Equation 2.15

By integrating the segmentation area and dividing by the time (Δt), the flux is [38]:

$$J = \frac{m}{A_s \Delta t} = \frac{1}{\Delta t}\int_{C_R}^{C^*}\left(x_f - x_i\right)\mathrm{d}C$$

Equation 2.16

Then, *Equation 2.16* is combined with Fick's law to obtain the interdiffusion coefficient [38]:

$$D = -\frac{1}{2}\left(\frac{\mathrm{d}x}{\mathrm{d}C_i} + \frac{\mathrm{d}x}{\mathrm{d}C_f}\right)\frac{\int_{C_R}^{C^*}(x_f - x_i)\,\mathrm{d}C}{\Delta t}$$

Equation 2.17

However, the Matano interface (x_M) is not included in this 2-profile BM equation. So *Equation 2.17* only applies when the Matano interfaces for both the initial and final profiles align.

2.2.3.2. 2-profile Sauer-Freise Equation

The normalized concentration ($Y = \frac{C^* - C_{-\infty}}{C_{+\infty} - C_{-\infty}}$) is inputted into *Equation 2.17* as follows [38]:

$$D = -\frac{1}{2}\left(\frac{dx}{dY_i} + \frac{dx}{dY_f}\right) \times \frac{\left[\left((1-Y^*)\int_{-\infty}^{x} Y\,\mathrm{d}x_f + Y^*\int_{x}^{+\infty}(1-Y)\,\mathrm{d}x_f\right) - \left((1-Y^*)\int_{-\infty}^{x} Y\,\mathrm{d}x_i + Y^*\int_{x}^{+\infty}(1-Y)\,\mathrm{d}x_i\right)\right]}{\Delta t}$$

Equation 2.18

In this study, *Equation 2.18* is used to eliminate computational errors from finding the Matano interfaces and reduce the computational workload for estimating the interdiffusion coefficients.

2.2.4. Temperature-dependent Interdiffusion Coefficient

Temperature dependence is another universally recognized characteristic of the interdiffusion coefficient. The equation for it is known as the Arrhenius equation, shown as follows [14, 39]:

$$D(T) = D_0 \cdot \mathrm{e}^{-\frac{Q}{RT}} = D_0 \cdot \mathrm{e}^{-\frac{Q}{k_B T}}$$

Equation 2.19

where the Q is the activation energy for diffusion, the R is the universal gas constant which is 8.314 joule/mol, k_B is the Boltzmann constant, and D_0 is the pre-exponential factor.

The interdiffusion coefficient has a positive correlation with temperature increases in most cases. By plotting $ln\,D$ against 1/T (Unit: K^{-1}), a straight line with $slope = -\frac{Q}{R}$ can provide the value of Q as long as the slope can be measured. The physical meaning of the pre-exponential factor D_0 and activation energy Q is related to the diffusion mechanism, diffusion process, lattice geometry, etc. However, these thermodynamic parameters are not the focus of this study.

2.2.5. Average Interdiffusion Coefficient

Unlike the concentration-dependent interdiffusion coefficient, which is typically plotted as a curve against concentration (the $\widetilde{D}(C)$ curve), the average interdiffusion coefficient (D_{Ave}) is a more comprehensible parameter for evaluating and comparing the interdiffusion behaviour.

The equation for calculating the average interdiffusion coefficient (D_{Ave}) is shown as follows:

$$D_{Ave} = \frac{\int_{C_L}^{C_R} D \,\mathrm{d}C}{C_R - C_L}$$

Equation 2.20

where C_R and C_L represent the concentration at the right end and left end of the compared zone.

This equation has been used as a more accessible means to evaluate interdiffusion behaviour. However, there are limitations since all the details within the $\widetilde{D}(C)$ are unknown, especially the concentration dependence. Therefore, it has only been used as an **auxiliary** of $\widetilde{D}(C)$ comparisons.

2.2.6. Forward Simulation Analysis

The FSA is a recently developed simulation method [10, 30, 32, 34] for estimating interdiffusion coefficients with a high degree of accuracy and obtaining impurity diffusion coefficients

simultaneously. The FSA is also a reliable method which can be used to validate the reliability of the code scripts used in this work.

The steps to implement an FSA are as follows:

i. The experimental concentration profiles are smoothened individually, and then their distance (x) data are averaged.
ii. An initial estimation of the interdiffusion coefficients is made by using BM or SF method.
iii. Based on the overall trends of the initial estimation, functions such as constant, linear, or quadratic functions can be assigned to the concentration profile.
iv. The concentration profile is simulated in a stepwise manner by using Fick's law of diffusion. In addition, the Boltzmann transformation [32], which is similar to the derivation of the BM equation, is utilized in the simulation process to improve algorithmic efficiency.

Dissimilar to the BM and SF equations, the forward simulation method does not require a "step-function" assumption for the initial concentration profile. Zhang and Zhao [32] determined the initial estimation by using the BM equation, but the estimation could be improved. Since the initial estimation only serves as the "initial guess anchor" for the simulation, a more accurate prediction closer to the actual results can reduce the simulation time. Changing the initial estimation would not change the accuracy and reliability of the final simulation results but only the simulation time required. Therefore, the BM equation can be replaced with the 2-profile SF in the modified code script. Overall, the FSA is a good method for validating the reliability of the 2-profile SF MATLAB® code script.

2.3. Time-dependence of Interdiffusion Coefficient

A number of reported data [1–10] inform that there could be an effect of diffusion time on interdiffusion coefficients. However, the focus of their investigation is not on time effect on $\widetilde{D}(C)$, which means that this time effect on $\widetilde{D}(C)$ has not been acknowledged/recognized in general.

2.3.1. Reported Data from Previous Studies

As mentioned above, previous studies have not focused on the time effect on interdiffusion coefficients. However, some of the data in the literature contradict conventional views that the interdiffusion coefficients do not depend on time, which has informed this work. Moreover, apart from the work of [10, 25], which was carried out by members of my research group, additional findings from the literature are provided, which also informed the investigation of this work.

In both [1] and [2], the cobalt-nickel (Co-Ni) diffusion couples were investigated with the BM method. The diffusion treatment times used in Kučera et al. [1] (1110°C) are 4 h, 9 h, 16 h, 36 h, and 49h, and the interdiffusion coefficients at 50 at% Co are 1.98×10^{-11} cm^2/s, 2.11×10^{-11} cm^2/s, 2.85×10^{-11} cm^2/s, 2.73×10^{-11} cm^2/s, 2.51×10^{-11} cm^2/s, respectively. The difference between the maximum and minimum values is about 43.9%. Similarly, in HŘebíček et al. [2] (1150°C) with the same diffusion treatment time, the interdiffusion coefficients at 50 wt% Co are 3.2642×10^{-11} cm^2/s, 2.9935×10^{-11} cm^2/s, 3.6331×10^{-11} cm^2/s, 6.0621×10^{-11} cm^2/s, 5.1848×10^{-11} cm^2/s, respectively. The difference between the maximum and minimum values is more significant.

In Badia and Vignes [3], the nickel/iron (Ni/Fe) system was investigated at relatively elevated temperatures. The Fe-Ni (70-30)/Fe diffusion couples were heated at 1136°C for 72 h and 95 h, which provided different interdiffusion coefficients with approximately a 9% difference. The

Fe/Co diffusion couples were also analyzed at the same temperature (1136°C). The diffusion time duration used in the diffusion experiments was 48.5 h and 116 h, thus resulting in different coefficient results of 8.9×10^{-12} m^2/s and 8.0×10^{-12} m^2/s, respectively, with a difference of 11.3%.

Opposits et al. [4] examined thin-film Cu-Ni diffusion couples, which were heated at 1223 K for 2.5 h, 5 h, 8.5 h, and 12 h. Using the BM method, they obtained the interdiffusion coefficients listed in *Table 2.1*. Although the diffusion system is also a Cu-Ni system [4], thin-film type diffusion couples were used instead of bulk-planar diffusion couples. Moreover, the study used the conventional 1-profile method (BM) instead of the 2-profile method for calculating the interdiffusion coefficient. They used electrodeposition to prepare the samples, which might create exceedingly refined grains. Meanwhile, the bulk planar samples were usually prepared by thermal bonding metal plates with sufficiently grown grains. Moreover, the focus of Opposits et al. [4] is diffusion-induced bending (macro deformation) of the thin films instead of the interdiffusion coefficient. Therefore, the work in [4] is not the same as the one done in this thesis.

In addition to a relatively short diffusion treatment time, a much longer diffusion treatment time should be considered for more robust results, as in Mehl [5]. For instance, the copper/aluminum (Cu/Al) system in Mehl [5] was heat treated at 700°C for 22.5 days and 37.5 days. As illustrated in *Figure 2.3*, the interdiffusion coefficient is not time-independent when the diffusion time is significantly longer. This is also the case with other studies that have used much longer diffusion treatment times [6–9].

The discussed data reported in the literature for time-varying concentration-dependent interdiffusion coefficients have informed the work in this thesis. However, unlike a previous study [10], this thesis is an experiment-based instead of a simulation-based project to validate the time effect on interdiffusion coefficients and investigate the most suggestive underlying factor(s).

Table 2.1 – Concentration-dependent Interdiffusion Coefficients from [4]

Time (h) T=1223K	$D(m^2/s) \cdot 10^{15}$ $C_{(Cu)}$ = 20 at%	$D(m^2/s) \cdot 10^{15}$ $C_{(Cu)}$ = 40 at%	$D(m^2/s) \cdot 10^{15}$ $C_{(Cu)}$ = 60 at%	$D(m^2/s) \cdot 10^{15}$ $C_{(Cu)}$ = 80 at%
2.5	2.0	3.3	5.3	5.4
5	1.3	2.2	3.3	10.2
8.5	0.8	1.2	2.5	8.7
12	1.6	1.5	3.2	8.6
Time Condition	2.5 h vs 8.5 h	2.5 h vs 8.5 h	2.5 h vs 8.5 h	2.5 h vs 5 h
Max Difference	1.2	2.1	2.8	4.8

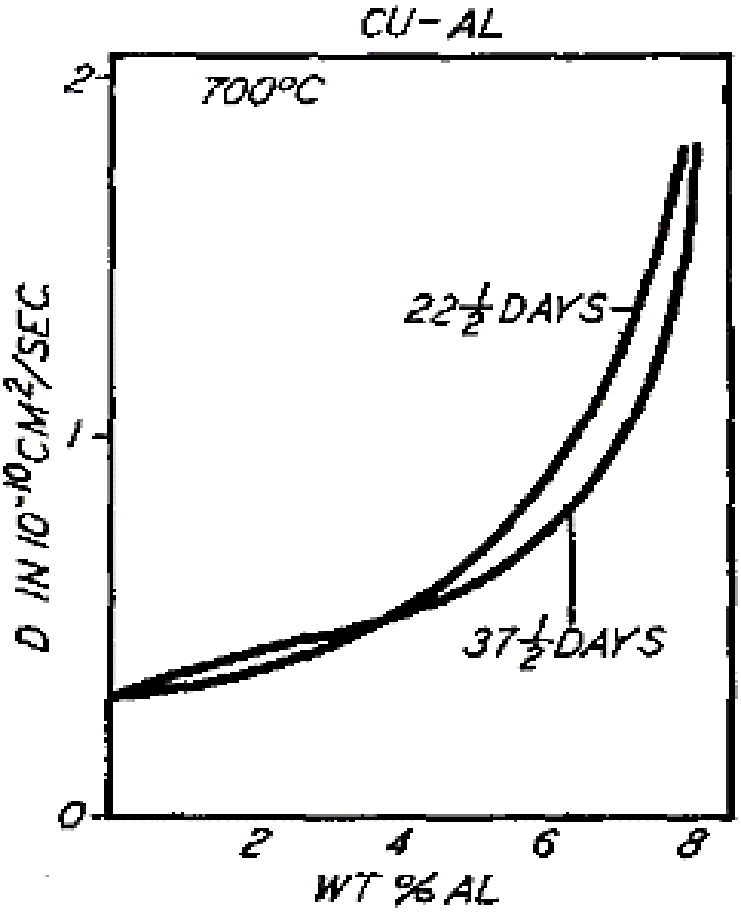

Figure 2.3 – Interdiffusion Coefficient Curves for α-phase in Al-Cu System from [5]

2.3.2. Potential Underlying Factor(s)

The reported data that agree with a time-varying $\widetilde{D}(C)$ have been discussed in the previous sections. Based on the literature review, the potential underlying factors of this time effect on interdiffusion coefficients are summarized as follows:

A. Pre-existing dislocations and/or stresses – in a diffusion system, these can act as an additional energy source or driving force that influences the interdiffusion process. However, with good sample preparation methods, these dislocations and/or stresses can be eliminated from a diffusion system, so they are entirely preventable.
B. The different microstructures in the diffusion systems - an example is the recrystallized refined grains due to cold work. However, the difference in microstructure can also be eliminated by using the appropriate sample preparation technique, particularly heat treatment at 1030°C for 4 h, as will be discussed in Chapter 3.
C. DIS - generated, relieved, and regenerated simultaneously in the diffusion system throughout the diffusion treatments. DIS is an intrinsic factor since it is initiated during the interdiffusion between dissimilar metals.

Factors A and B can be prevented since it is possible to eliminate them by controlling the experimental parameters. Meanwhile, Factor C is intrinsic [4, 11, 25, 28], which means that this factor cannot be eliminated by merely controlling the parameters in an experiment. More importantly, there have been studies [18, 20, 24] that conclude on its ability to influence the interdiffusion coefficients, and studies [10, 25] show that the interdiffusion coefficients can change with $\frac{\partial C}{\partial X}$ if the DIS is present in the diffusion system.

2.3.2.1. Types of Diffusion in Polycrystalline Binary System

An introduction on volume diffusion and grain boundary diffusion (**GBD**) and their relationships with the interdiffusion coefficients will be given in this section to provide a more comprehensive discussion of how the factor B can be eliminated and avoided.

When performing an experimental interdiffusion coefficient analysis in a polycrystalline couple, there are two forms of diffusion: volume diffusion and grain boundary diffusion (GBD). The former is defined as the transfer of atoms within each crystal grain or between two grains in the direction normal to the grain boundary, as shown in *Figure 2.4*. Meanwhile, GBD is the mass transfer along the grain boundaries, also shown in *Figure 2.4*. The equation to calculate the volume diffusion and GBD [29] is shown as follows:

$$D_{exp} = D_v + f \cdot D_{GB}$$

Equation 2.21

where the D_{exp} is the experimentally determined interdiffusion coefficient, the D_v is the volume diffusion coefficient, the D_{GB} is the GBD coefficient, and the f is a geometric factor that depends on the microstructure ($f \geq 0$).

Volume diffusion is the focus when utilizing planar bulk diffusion couples (as in the case of this thesis). When the grain boundary area per unit volume is relatively small, the geometric factor f tends towards zero, which makes the GBD negligible [41]. Although a monocrystalline diffusion couple can maintain a low geometric factor f, preparing such metals is expensive and time-consuming. Thus, the monocrystalline diffusion couples are not used in this study.

On the contrary, the nanocrystalline/microcrystalline condition (e.g., thin-film diffusion couple prepared by electrodeposition [4]) is more suitable for analyzing the GBD since the grain boundary area per unit volume is much larger. Therefore, the recrystallized refined grains due to cold work could be an ideal condition for GBD.

The GBD can have a considerable influence on planar bulk diffusion couples. According to [41–43], the high volume-fraction of grain boundaries can quickly facilitate atomic diffusion compared to the one with coarse grain boundaries. Suppose the grain boundary area per unit volume is large (viz. when the factor f is not negligible); since the GBD takes place in a large area, this can result in a higher estimation of the effective interdiffusion coefficients.

The diffusion treatment temperature in this study is relatively high, and the GBD tends to be lower at elevated temperatures [41]. This means the geometric factor f becomes negligible (the volume diffusion coefficient becomes predominant) when the diffusion treatment temperature is high while the grain size is large. For this study, the grain size should be large enough (based on the estimation in the study [44]) with heat treatment that comprises recrystallization, stress relief and grain growth at 1030°C for 4 h before thermal bonding.

2.3.2.2. Diffusion-induced Stress

DIS emerged as a study topic a few decades ago, but the related studies did not initially focus on its influence on interdiffusion coefficients. One of the first studies to discuss DIS was done by Prussin [45] and published in October 1961. The study addressed the stress and dislocations induced by diffusion in a silicon wafer. However, the interdiffusion coefficients were expected to remain constant in the study since the concentration profile was characterized by a complementary "error function" (erf) distribution mentioned in Section 2.2.1.

With time, more studies [4, 11–14, 20, 22, 23, 28, 41, 45] about DIS have been published. *Figure 2.5* shows the correlations among volume diffusion, DIS, and relaxation of DIS. The correlations are discussed as follows.

Due to the imbalance of mass transfer, volume diffusion can cause micro-scale deformation, which accumulates and forms DIS. The generation of DIS is somewhat intrinsic/inevitable due to the mass transfer between dissimilar atoms. In this way, the stress can potentially build up in the diffusion system, thus initiating micro/macro deformation (such as the Kirkendall shift and bending of the thin films) and changes in thermodynamic potential, which acts as an additional source of driving force for interdiffusion.

Moreover, the relaxation of DIS does not happen at the same rate as the generation of DIS, which means that the former is not rapid enough to offset the DIS immediately. As a result, the DIS can accumulate near the interface of dissimilar metals. Furthermore, according to [25], the relaxation rate of DIS is related to the viscosity of the diffusion system. This means that factors like the compositions/elements of the diffusion system, diffusion treatment temperatures, etc., can influence the DIS by changing the viscosity of the diffusion system. Overall, micro/macro deformation and stress-induced diffusion can occur [20, 24] due to the presence of DIS.

2.3.2.3. Changes in Driving Forces

DIS can alter the thermodynamic potential of interdiffusion, as previously mentioned. Thus, the related information is included in this section, especially the driving forces of interdiffusion.

Generally speaking, the chemical potential gradient ($\nabla\mu_{Chemical}$) is the only gradient considered. However, a number of studies have revealed that there are more gradients are included, as shown

in *Equation 2.22* [18, 20, 24], which means that multiple driving forces could be present at the same time in a diffusion system:

$$\frac{\partial C}{\partial t} = D \cdot \nabla\left(\nabla\mu_i \,\&\, \nabla\mu_j \,\&\, \ldots\right)$$

Equation 2.22

Apart from $\nabla\mu_{Chemical}$, other gradients, such as the electropotential gradient ($\nabla\mu_{Electrical}$) from the external electric field, thermal-potential gradient ($\nabla\mu_{Thermal}$) due to non-uniform heating, magnetic-potential gradient ($\nabla\mu_{Magnetic}$) from the external magnetic field and mechanical (stress) potential gradient ($\nabla\mu_{Mechanical}$) have been taken into consideration in many studies. Since the diffusion system is free of the thermal, electrical and magnetic fields in this study, *Equation 2.22* can be derived into an elastochemical form, as shown in *Equation 2.23* [18, 20, 24]:

$$\frac{\partial C}{\partial t} = D \cdot \nabla(\nabla\mu_{Chemical} \,\&\, \nabla\mu_{Mechanical})$$

Equation 2.23

where $\nabla\mu_{Chemical}$ is the chemical potential gradient and the $\nabla\mu_{Mechanical}$ is the mechanical potential gradient, possibly due to the internal stress (DIS) in an (external) stress-free condition.

Typically, the diffusion flux is always in the direction of the decreasing potential in a system. Since the atoms have higher chemical potential when their concentration is higher, especially for a simple binary system without complex interactions (e.g., without the occurrence of up-hill diffusion), the $\nabla\mu_{Chemical}$ can be interpreted as ∇C or $\frac{\partial C}{\partial x}$ (concentration gradient in space).

Even though the correlation between the interdiffusion coefficient and potential gradients appears to be simple and straightforward in *Equation 2.23*, in fact, the generation and relief of DIS are highly complex processes [23, 46]. However, providing the theoretical basis behind this

phenomenon is not the focus of this study. Therefore, an equation for deriving the complex relationship between DIS and the driving forces is not included (*Equation 2.23* is only a qualitative expression).

Even though the exact equation will not be included, other factors can still show the complexity of DIS. For instance, due to the imbalance of stress relaxation, the plotted distribution of DIS could show a sharp peak at one side near the interface of dissimilar metals [14, 19]. In addition, the distribution of DIS depends on many factors, such as the boundary conditions (geometry) of diffusion couples and the viscosity of the diffusion system [25]. Moreover, the generation, relaxation and regeneration of DIS could happen simultaneously at different rates [24]. As one of the processes that cause stress relaxation, the Kirkendall shift is often slow and incomplete, which results in stress relief and the appearance of a DIS field gradient at the same time.

Due to technical limitations, a precise and real-time measurement of the DIS can be quite challenging at present. Although the magnitude of DIS can be generally estimated based on the diffusion-induced bending of thin-film samples [23, 46], this estimation cannot provide sufficient details. More importantly, it is not applicable to bulk planar diffusion couples as in this study.

Thus, an indirect way to investigate DIS is required. The $\frac{\partial C}{\partial x}$ is a directly measurable parameter, and more importantly, apart from the studies [28] showing the strong correlation between $\frac{\partial C}{\partial x}$ and DIS, studies [10, 25] have shown that interdiffusion coefficients can change with $\frac{\partial C}{\partial x}$ due to the presence of DIS. Thus, with the general acknowledgement that $\frac{\partial C}{\partial x}$ changes with diffusion time in isothermal diffusion, the $\frac{\partial C}{\partial x}$ can be used as an indirect approach for validating whether DIS is the most suggestive underlying factor of time effect on interdiffusion coefficients.

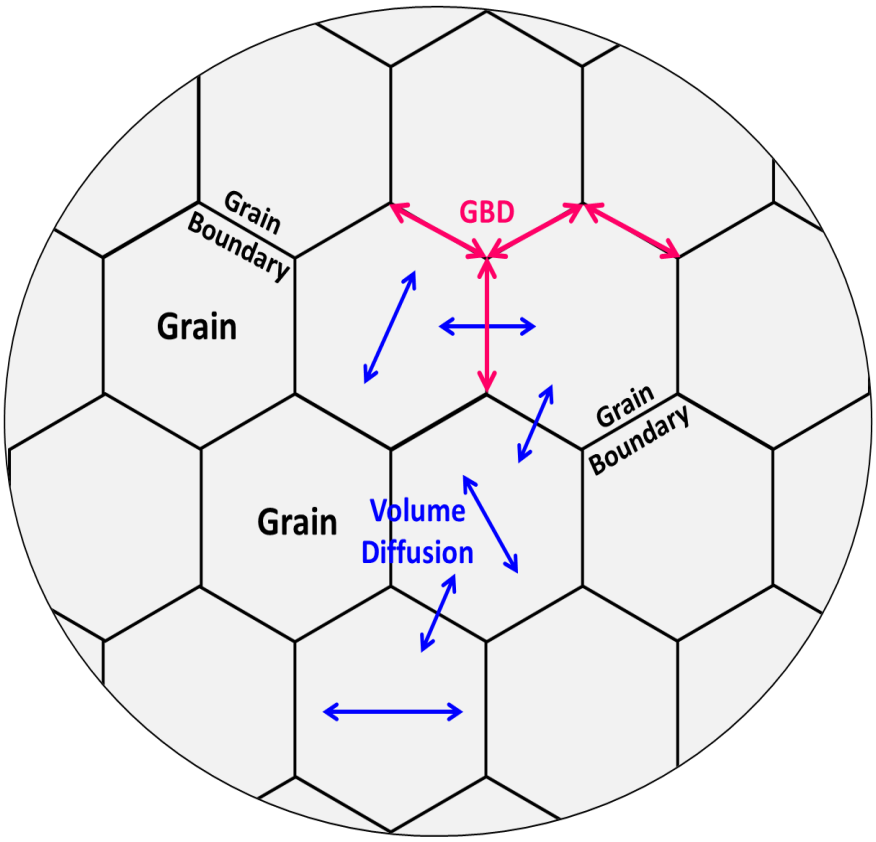

Figure 2.4 – Volume Diffusion and Grain Boundary Diffusion

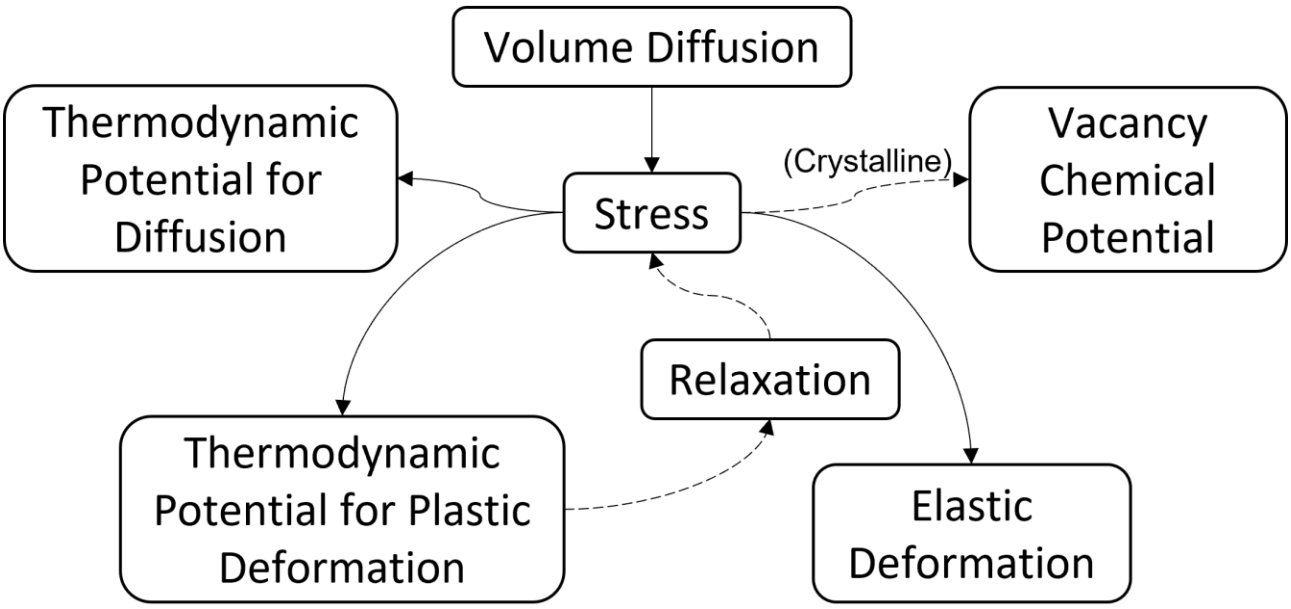

Figure 2.5 – Scheme of the DIS in a Binary System from [11]

3. Methodology

3.1. Raw Materials

The raw materials used in this study are as follows: pure Cu, pure Ni and a $Cu_{90}Ni_{10}$ alloy (a Cu-based alloy with 10 at% Ni), all of which were purchased from *ACI Alloys Inc*. (USA). The details are listed in *Tables 3.1* and *3.2*. The homogenization of the $Cu_{90}Ni_{10}$ alloy is essential since the measured concentration profile is the focus. To shorten the required homogenization treatment time, the alloy plates were cold-rolled down to 40% of their original thickness to provide additional energy and sufficient dislocations. Then these alloy plates were heat-treated at 1030°C (1303K) for 75 h in vacuumed quartz capsules with backfilled argon (Ar) gas.

3.2. Methods of Sample Preparation

An introduction of the preparation processes of the diffusion couple and metallography samples is provided in this section. It is crucial to keep the consistency of these processes.

3.2.1. Heat Treatment of Raw Materials

Before thermal bonding, all the metal plates were cold-rolled to approximately 1.5mm in thickness using a rolling machine. As such, they are thin enough for the thermal bonding jigs shown in *Figure 3.1*. However, the metal plates contain a large number of dislocations and stresses, which can influence interdiffusion. These dislocations and grain boundaries can act as high-diffusivity pathways due to the higher mobility of atoms along with defects than in the lattice [41–43]. Therefore, sufficient stress relief and grain growth treatments are necessary before thermal bonding takes place. The metal plates were encapsulated in quartz capsules and then heat-treated

at 1030°C for 4 h, which is a high enough temperature to trigger recrystallization and stress relief. Generally speaking, recrystallization and stress relief should be completed after 60 min of isothermal heat treatment at or above the initiation temperature. Also, the minimal time required decreases with increasing temperatures.

In addition, the grain size needs to be large enough to minimize the grain boundary area per volume. However, a long period of heat treatment would not result in observable grain growth. Even at lower temperatures, such as heat-treating Cu at 280°C, the average grain size does not increase considerably after 60 min [47]. Therefore, the heat treatment temperature (1030°C) and time (4 h) are sufficient in this study.

3.2.2. Thermal Bonding of Dissimilar Metals in Planar Binary System

Pure Cu and Ni have a passivated layer that covers their surface, thus inhibiting the thermal bonding and further influencing the diffusion treatment. Therefore, the surface preparation process must be capable to fully expose the underlying metal surface for thermal bonding. The samples were subsequently grinded with sandpapers (240, 600 and 1200 grit) and polished by using diamond suspensions. In addition, the samples were subjected to a thorough ultrasound cleaning after being grinded with sandpapers to prevent bringing SiC particles from sandpapers to the fine polishing sequence with diamond suspensions (3 μm and 1 μm). Finally, a *NICROBRAZ Green Stop-off Pen Type 1* was used to evenly apply a solvent-based material on the back side of polished samples to prevent adhesion between the steel jigs and diffusion couples.

In terms of industrial diffusion bonding processes, the thermal bonding procedure requires a load from the jig plates [42]. As shown in *Figure 3.1*, each bolt is tightened until the resistance torque is 15- 20 ft·lbs. Then, *Equation 3.1* is used to convert the torque to the axial load applied to the

samples, which is 53 - 71 kN from each bolt. Thus, the total load applied to the diffusion samples is 212 - 284 kN to ensure a compacted contact between the dissimilar metals.

$$T = k \cdot F \cdot \mathrm{d}\frac{1 - L}{100}$$

Equation 3.1

where T is the torque (ft·lbs), k = 0.2 is a dimensionless ratio for a regular dry surface, d is the nominal bolt diameter (m), F is the axial load (N), and L is the lubrication factor (%).

Thermal bonding was carried out in a brazing furnace (*GCA corporation Vacuum Industries Division*) at 600˚C for 1 h under a high vacuum of approximately 1×10^{-8} PSIG.

3.2.3. Electrodeposition to Prevent Oxidation

After thermal bonding took place, the diffusion couples were subjected to an electrodeposition process to enhance the oxidation resistance during the diffusion treatments.

First, the surface of all of the samples were subjected to cleaning and then activating process with chemicals including an alkaline mixture (NaOH, Na_2CO_3, and Na_2HPO_4) solution, HCl and H_2SO_4 acid solution before the electrodeposition. The activating process with a diluted H_2SO_4 acid solution is essential, or the protective coating cannot form a firm bond with the diffusion couples.

Afterward, the samples were transferred to a glass vessel and immersed in an electroplating solution ($NiSO_4 \cdot 6H_2O$, $NiCl_2 \cdot 6H_2O$, and H_2BO_3). The current is proportional to the surface area of the samples: 10 mA/cm^2, which is provided by *VersaSTAT3 Potentiostat Galvanostat*. The saturated calomel electrode (SCE) served as the reference electrode, the anodic electrode is a pure Ni bar, and the cathodic electrode is the diffusion sample to be plated. The electrodeposition time required to obtain a firm protective coating is 8000 s.

Table 3.1 – Components of Planar Binary System

Diffusion Couple	Material A	Material B
Planar Pure Element System	Pure Cu	Pure Ni
Planar Alloy System	$Cu_{90}Ni_{10}$ Cu-based Alloy	Pure Ni

Table 3.2 – Concentration of Raw Materials

Material	Cu at%	Ni at%
Pure Cu Plate	100.00	–
Pure Ni Plate	–	100.00
$Cu_{90}Ni_{10}$ Alloy Plate	88.92 ± 0.35 (89)	11.08 ± 0.35 (11)

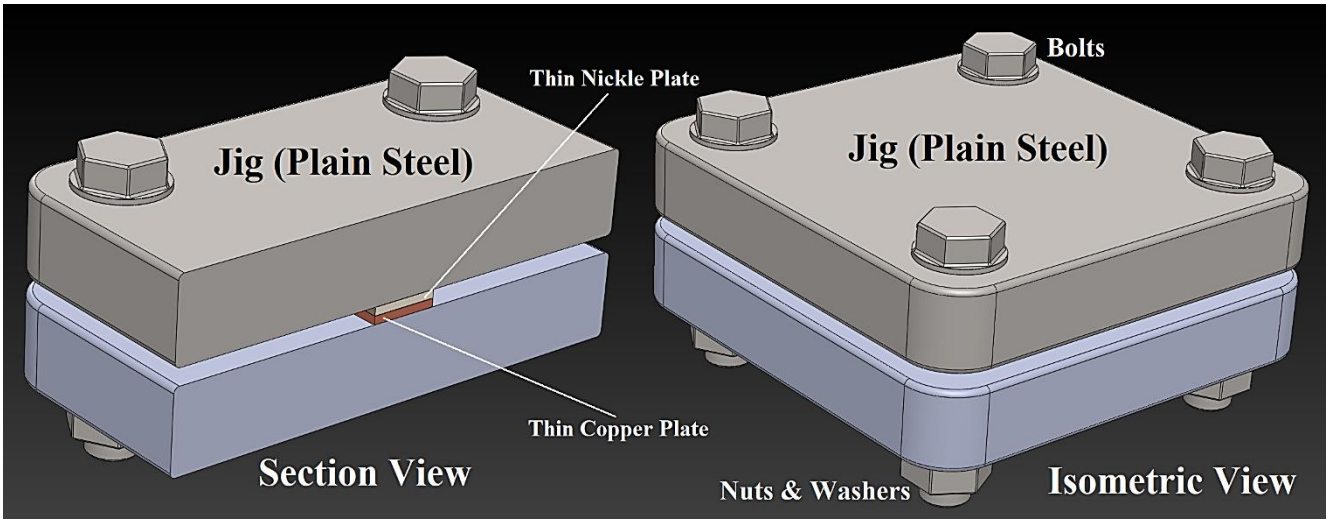

Figure 3.1 – Isometric and Section View of Thermal Bonding Apparatus (Jigs)

3.2.4. Isothermal Diffusion Heat Treatments

After electrodeposition, all of the bulk planar samples were encapsulated in vacuumed quartz capsules with backfilled Ar gas. Then, the following diffusion treatments were carried out:

i. Single-stage diffusion treatment in Cu-Ni and $Cu_{90}Ni_{10}$-Ni systems:
    a. At 900°C for 5, 25, 75, and 150 h.
    b. At 950°C for 5, 25, 75, and 150 h.
    c. At 1000°C for 5, 25, 75, and 150 h.

ii. Two-stage diffusion treatments in the Cu-Ni system:
    a. First/initial stage: Pre-existing non-uniform solute distribution Type A. The heat treatment is performed at 900°C for 5 h.
        - Second/final stage: 950°C for 0 h (as-bonded), 5 h, 25 h, 75 h, and 150 h.
    b. First/initial stage: Pre-existing non-uniform solute distribution Type B. The heat treatment is performed at 1000°C for 5 h.
        - Second/final stage: 950°C for 0 h (as-bonded), 5 h, 25 h, 75 h, and 150 h.

iii. A longer diffusion treatment at 900°C for 450 h in the Cu-Ni system.

The quartz tubes might undergo devitrification when heat-treated at elevated temperatures for a prolonged period of time, which can reduce their mechanical strength. In addition, water cooling these capsules can have similar consequences. These quartz capsules might burst if they become too fragile. This is hazardous to both the furnace and the users. All of the quartz capsules were therefore wrapped with stainless steel heat treatment foil to prevent damage/injury due to bursting fragments, and water cooling was replaced with air cooling.

3.3. Methods of Data Measurement

The diffusion treatment samples were sectioned by using an electric discharge machine (EDM) and then hot-mounted in bakelite. Next, the standard preparation procedures for metallography samples were performed. After that, they were subjected to a visual inspection under OM to ensure that their surfaces were clean and free of particles. Then, concentration profiles were measured by using EDS in *JEOL JSM-5900LV SEM*.

The resolution of the EDS measurement is around 1 μm [48] due to the inherent property of the electron-matter interaction volume. Due to this limitation, the concentration profile must meet 1 at% per minimal 1 μm for a reliable result. Therefore, the minimal measurable diffusion penetration depth of the Cu-Ni system (0 - 100 at%) is 100μm. Empirically, each intact profile needs at least 50 data points that range from 0 at% to 100 at% to obtain an adequate measured concentration profile, thus preventing either undersampling or oversampling.

3.4. Data Smoothing and Analysis Methods

Before calculating the interdiffusion coefficient, the discrete data noise in the measured concentration profile must be removed through a data smoothing process which involves both the SMA and PCHIP.

3.4.1. Simple Moving Average

The measured experimental data can contain discrete noise, which affects the calculation of the interdiffusion coefficients, so the data cannot be directly used. To address this issue, previous studies [32, 36, 48] have used both an SMA algorithm and spline/PCHIP interpolation. The

equation for the SMA algorithm is as follows. In MATLAB®, the default moving average has a two-sides (*Equation 3.2* [37]):

$$\hat{f}(t) = \frac{1}{2k+1}\sum_{j=-k}^{k} y_{t+j}\,, \qquad t = k+1, k+2, \ldots, n-k.$$

Equation 3.2

where $y_1, \ldots, y_n$ is the original data series, and $\hat{f}(k+1), \ldots, \hat{f}(n-k)$ is the new data series.

The idea is to shift the neighboring discrete data points based on the estimation of the overall trend. The SMA algorithm reduces randomness and smoothens the data. Afterwards, the PCHIP interpolation function is applied to generate smoothened concentration profile for calculating the interdiffusion coefficients. A comparison between the PCHIP and spline function in MATLAB® [35] shows that the PCHIP can provide a more accurately smoothened outcome of the Cu-Ni concentration profile. So, the PCHIP is used instead of spline interpolation in this study.

3.4.2. Averaging Measured Concentration Profiles

The average smoothed concentration profile should be in the center of the experimental data dot "cloud" by sectioning half of the data points on either side of the curve, similar to the smoothing outcomes in studies [32, 36, 48].

The standard procedure for smoothening and averaging the data is as follows:

i. There are six measured concentration profiles from each sample. All of them were individually smoothened and then realigned based on their Matano interfaces. It is recommended that they should not be overly smoothened to prevent loss of details.

ii. All of the concentration profiles are aligned based on their Matano interfaces, and the distance of each concentration point for all six profiles is averaged. ($\sum_{i=1}^{n} x_i \,/\, n = (x_1 + x_2 + x_3 + x_4 + x_5 + x_6) \,/\, 6$).

iii. The average concentration profile is further smoothened. This step is recommended so that the calculation results – plotted $\widetilde{D}(C)$ curves contain less waves.

To obtain a better-looking plotted $\widetilde{D}(C)$, the "point skipping" in Origin®Lab can be used, which does not impact the calculation of the average interdiffusion coefficient. On the contrary, smoothing the $\widetilde{D}(C)$ curves directly might severely impact the calculation outcomes.

3.5. Reliability Verification of Experimental Data

The diffusion treatments were repeated to demonstrate the reliability of the experimental data and obtain the range of uncertain values. Only two specific conditions were repeated for efficiency of time and cost.

Each condition has 3 diffusion couples to determine the range of uncertain values. Six (6) concentration profiles were measured from each diffusion couple, which means that there are 18 concentration profiles in total for each repeated condition. As a result, the range of uncertain values, as shown in *Table 3.3*, is much lower than the empirically determined uncertainty (15%), which means that the experimental results have high reliability. Meanwhile, the *p*-values of the *t-statistics*, which will be discussed in detail in Section 3.6, statistically validate the reliability.

Moreover, the error bars of a single versus all three samples show some minor differences. Comparisons among 1 and 3 diffusion samples are shown in *Figure 3.2*, which shows nearly the same results with less than a 5% difference. Therefore, the obtained experimental data are considered to be reliable.

Table 3.3 – Range of Uncertainty

	$D_{Ave,Min}$	Difference & p	$D_{Ave,mean}$	Difference & p	$D_{Ave,Max}$
5-150 h	4.053E-15	6.69% p>>0.2	4.324E-15	7.00% p>>0.2	4.626E-15

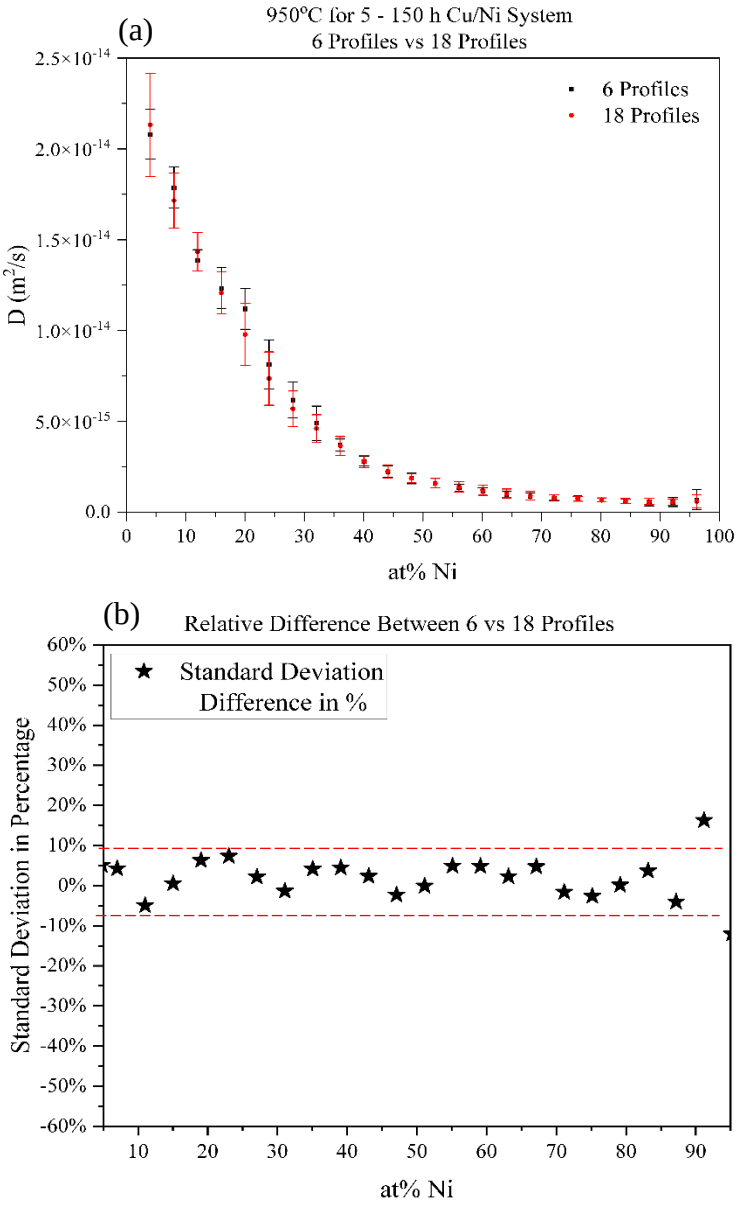

Figure 3.2 – Reliability Check with Error Bars

3.6. Two Samples Statistical Test (*t-statistics*)

Since the error bars and difference of D_{Ave} in percentage are either visual or empirical indicators, a statistical/mathematical assessment is required. The test statistic (*t-statistics*) is one of the most commonly used approaches:

$$t = \frac{|D_1 - D_2|}{\sqrt{\frac{s_1^2}{n_1} + \frac{s_2^2}{n_2}}}$$

Equation 3.3

where *t* is the test statistic (*t-statistics*) value for determining the *p*-value, D_1 and D_2 are the mean value of the interdiffusion coefficients for two conditions, S_1 and S_2 are the standard deviations of D_1 and D_2, and n_1 and n_2 are the amount of data we acquired.

The degree of freedom is included to find the row of A/P indicators from the *t*-distribution A/P table. The equation is shown as follows:

$$DOF = n_1 + n_2 - 2$$

Equation 3.4

where *DOF* is the degree of freedom, and n_1 and n_2 are both 6. Therefore, the degree of freedom is 10 in this case.

The recommended benchmark is $p<0.05$. Therefore, the difference/separation is statistically reliable when $p < 0.05$. On the other hand, when $p > 0.2$, the compared data sets can be considered to be the same. The experimental data sets are in the quasi-normal distribution, which means that the *t-statistics* is applicable to this work.

4. Results and Discussion

This chapter presents the results and discussion on the isothermal interdiffusion treatment. Error bars are used to graphically show the variations in the interdiffusion coefficients. Meanwhile, the *p*-values are included as statistical indicators to show the reliability of these variations. Additionally, the differences in percentage are used to explicitly identify the variations in D_{Ave}.

4.1. Verification of Time Effect in Cu-Ni System

To verify the occurrence of time effect on the interdiffusion coefficient, comparisons are carried out among isothermal diffusion treatments with specific time intervals at the same temperature. The time intervals used for comparisons, in general, are 5-25 h (a 20 hours period), 25-75 h (a 50 hours period), and 75-150 h (a 75 hours period). The 150 - 450 h (a 300 hours period) is a specific interval which is only carried out at 900°C.

4.1.1. Verification of Time Effect at 900°C in Cu-Ni System

Figures 4.1 - 4.3 are the plots of the interdiffusion coefficients for each concentration point from 5 to 95 at% Ni ($\widetilde{D}(C)$ curves) at 900°C for different time intervals of diffusion. Usually, the interdiffusion coefficient does not depend on the diffusion time, which means that there should be no apparent variation of the interdiffusion coefficients with diffusion time.

However, the differences in the interdiffusion coefficients between the shorter and longer diffusion treatment $\widetilde{D}(C)$ curves are obvious, as highlighted by the red/blue circles in *Figures 4.1 (c)* and *4.2*. Moreover, as shown in *Table 4.1*, the *p*-values of the *t-statistics* are mostly smaller than the

recommended benchmark (p<0.05), which means that these differences are statistically valid. Therefore, undoubtedly, $\widetilde{D}(C)$ can change with diffusion time at 900°C in the Cu-Ni system.

In addition, the variations of the $\widetilde{D}(C)$ curves and error bars are more evident on the left side (7 - 51 at% Ni) of these plots, which means that such variations are more substantial in the Cu-rich interdiffusion region. This could be a potential characteristic of the time effect on the interdiffusion coefficient – that there is a tendency for variation in the interdiffusion regions with more Cu.

Meanwhile, as stated earlier, the D_{Ave}[a] is a more straightforward indicator to show the significant differences between shorter and longer diffusion treatments, as shown in *Table 4.2*. The observable variations (approximately a 100% increase) against diffusion time in D_{Ave} are also contrary to the conventional recognition that the interdiffusion coefficients are not dependent on diffusion time since all of the differences in percentage are much higher than the empirically derived benchmark.

As mentioned earlier, another longer diffusion treatment was carried out at 900°C for 450 h (18 days and 18 hours). The $\widetilde{D}(C)$, p-values of the *t-statistics* and the D_{Ave} results are shown in *Figure 4.3* and *Tables 4.1* and *4.2*. The variations in $\widetilde{D}(C)$ and D_{Ave} are still noticeable after this longer diffusion treatment time. Similar time-varying interdiffusion coefficients for longer diffusion treatment times can be found in [5–9], which have informed the one in this work.

The results showed that the interdiffusion coefficient is **NOT** isothermally constant against diffusion time in the Cu-Ni system at 900°C. In addition to a temperature of 900°C, different temperatures (950°C and 1000°C) were taken into consideration to conduct a more comprehensive investigation. The results are presented in the following sections.

[a] The equation for difference of average interdiffusion coefficient in percentages: $D_{Ave}^{in\ \%} = \frac{D_{Ave}^{High} - D_{Ave}^{Low}}{D_{Ave}^{Low}}$

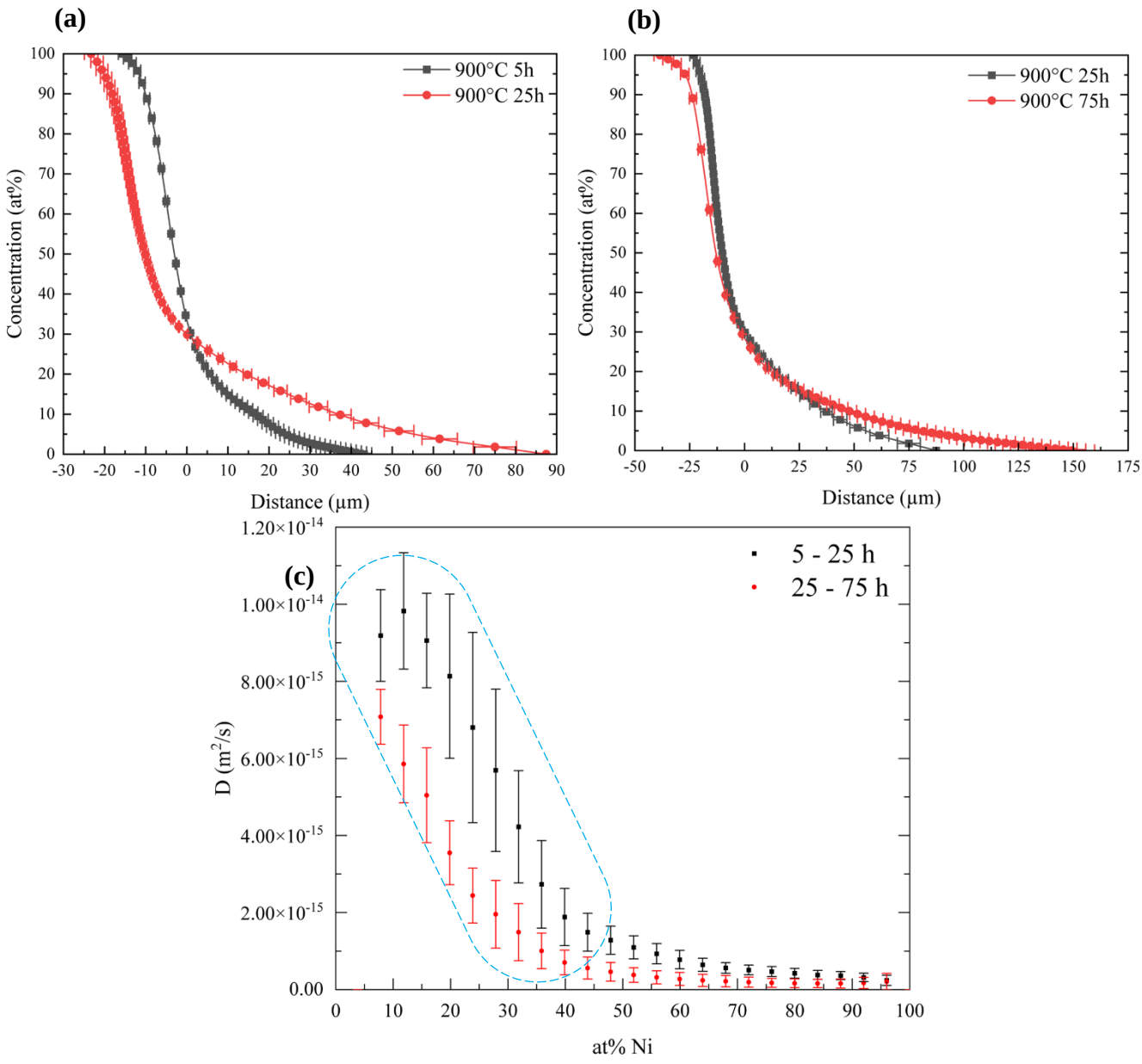

Figure 4.1 – Concentration Profiles (a) 5-25 h and (b) 25-75 h and (c) Interdiffusion Coefficient for Cu-Ni System at 900°C for 5-25 h vs. 25-75 h

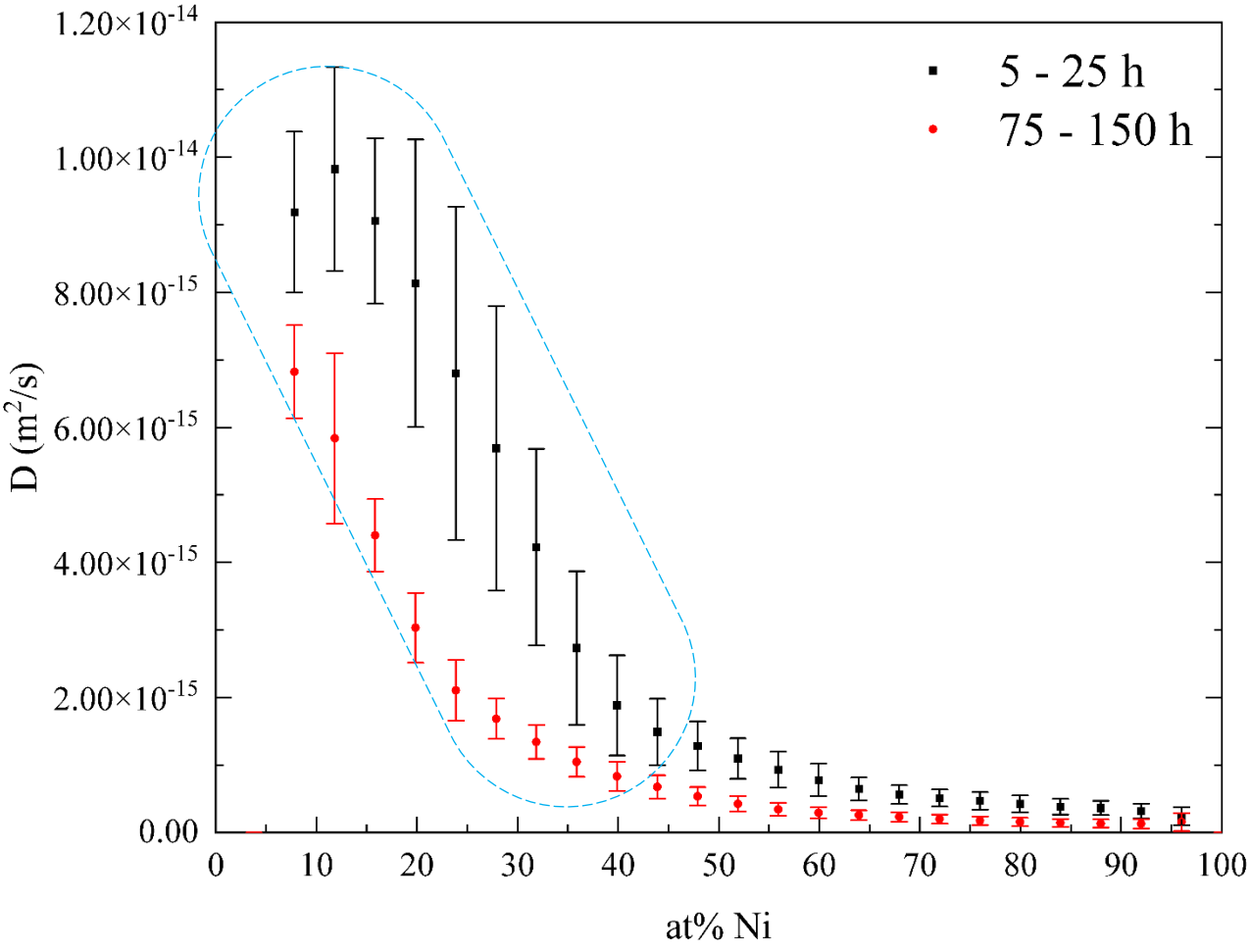

Figure 4.2 – Interdiffusion Coefficients for Cu-Ni System at 900°C for 5-25 h vs. 75-150 h

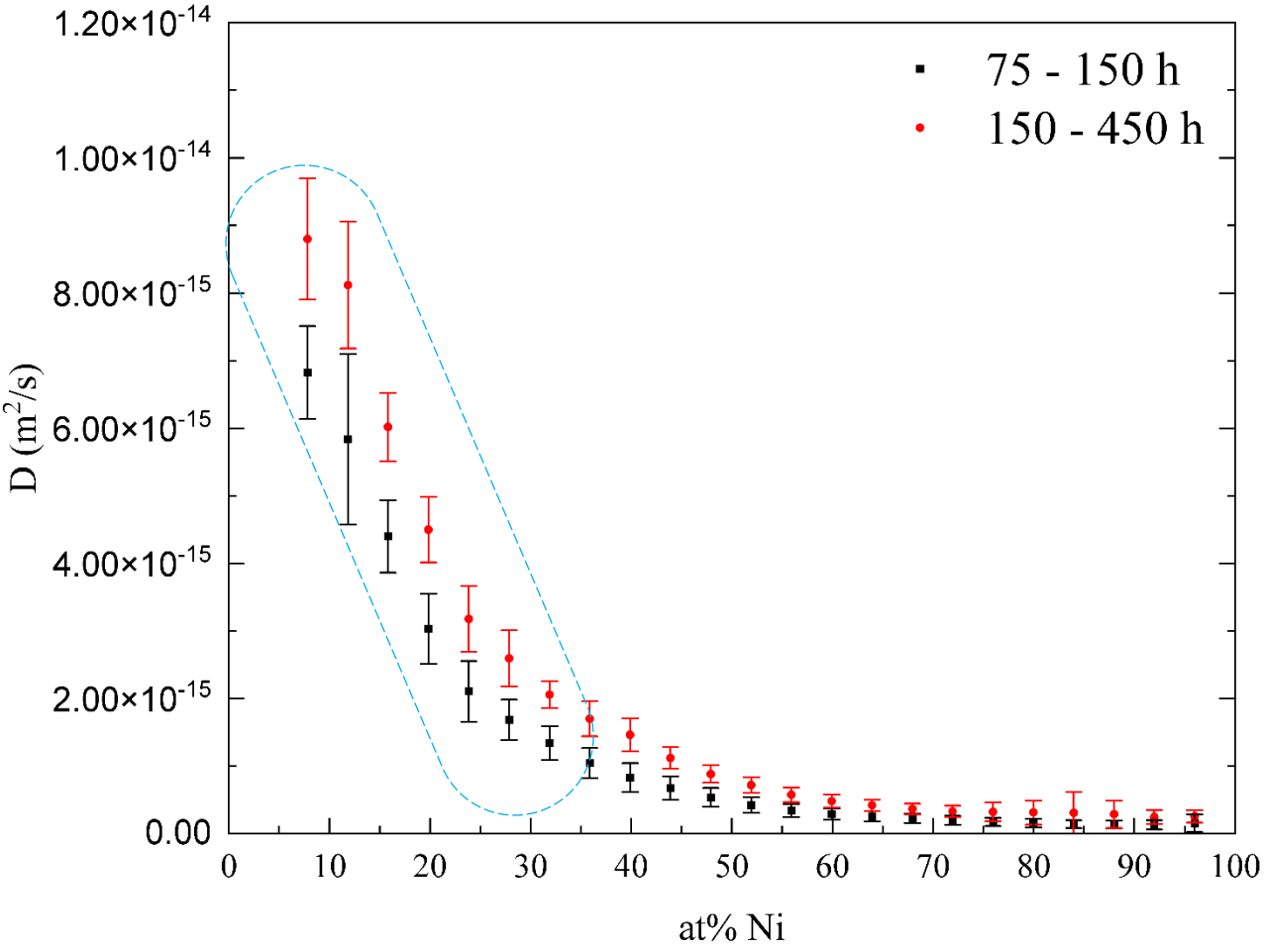

Figure 4.3 – Interdiffusion Coefficients for Cu–Ni System at 900°C for 75-150 h vs. 150-450 h

Table 4.1 – *p*-values of the *t-statistics* for Cu-Ni system at 900°C

Ni at%		7.0 - 31.0							
75-150 h vs 150-450 h	p								
5-25 h vs 75-150 h	p	≤0.001							
5-25 h vs 25-75 h	p								
Ni at%		35.0 - 63.0							
75-150 h vs 150-450 h									
5-25 h vs 75-150 h		≤0.001							
5-25 h vs 25-75 h									
Ni at%		67.0	71.0	75.0	79.0	83.0	87.0	91.0	95.0
75-150 h vs 150-450 h		0.002	0.005	0.02	0.05	0.200	0.100	0.05	0.100
5-25 h vs 75-150 h		0.001	0.001	0.001	0.001	0.001	0.001	0.001	0.100
5-25 h vs 25-75 h		0.001	0.001	0.001	0.001	0.001	0.002	0.05	>>0.2

Table 4.2 – Average Interdiffusion Coefficients for Cu-Ni System at 900°C

Time Intervals	25-75 h	Difference in Percentage	5-25 h	Difference in Percentage	75-150 h	Difference in Percentage	150-450 h
$\boldsymbol{D_{Ave}}$ (m^2/s)	1.5484E-15	+98.82% ✓	3.0785E-15	+109.57% ✓	1.4690E-15	+44.86% ✓	2.1280E-15
p	–	< 0.001	–	< 0.001	–	< 0.001	–

4.1.2. Verification of Time Effect at 950°C in Cu-Ni System

In addition to the temperature of 900°C, a temperature of 950°C was also taken into consideration to verify that there is a time effect on the interdiffusion coefficient. The plotted $\widetilde{D}(C)$ curves with error bars that compare shorter and longer diffusion times at 950°C are shown in *Figures 4.4* and *4.5*. Meanwhile, the D_{Ave} results and their differences in percentage are presented in *Table 4.4*.

The D_{Ave} results show variations with diffusion time. Compared with the result for a time interval of 5-25 h, that for 25-75 h is 24.49% higher, and the one for 75-150 h is 15.59% higher. The difference in percentage for both compared time intervals is greater than the empirically derived 15%, but the corresponding $\widetilde{D}(C)$ curves with error bars show less variation. *Figures 4.4* and *4.5* show that only a few concentration points, such as 7, 11, and 15 at% Ni, have noticeable differences. Meanwhile, the *p*-values of the *t-statistics* in *Table 4.3* also show a similar result with only a few concentration points that have a *p*-value less than the benchmark (p<0.05). A comparison between the time intervals of 25-75 h and 75-150 h was also carried out but not presented since both the $\widetilde{D}(C)$ curves and D_{Ave} results are almost the same. Therefore, only a very small range of concentration can be found to have a time effect on the interdiffusion coefficient at 950°C. The time effect appears to be more noticeable in the early stages of the interdiffusion.

Overall, the time effect on the interdiffusion coefficient is less apparent but still detectable at 950°C in the Cu-Ni system. A subsequent set of diffusion treatments were carried out to further determine if the time effect has an impact at 1000°C; the results are provided in the next section.

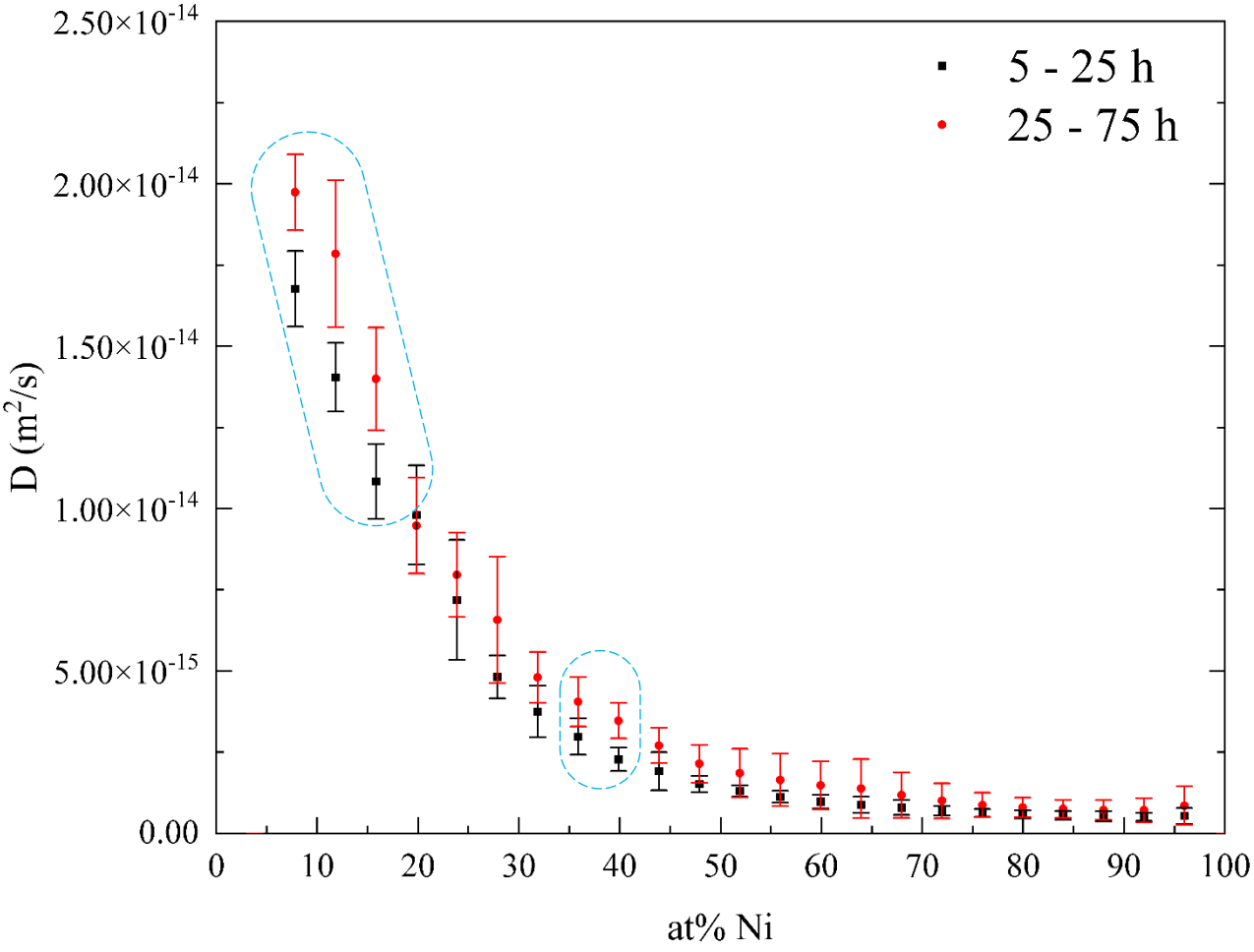

Figure 4.4 – Interdiffusion Coefficients for Cu-Ni System at 950°C for 5-25 h vs. 25-75 h

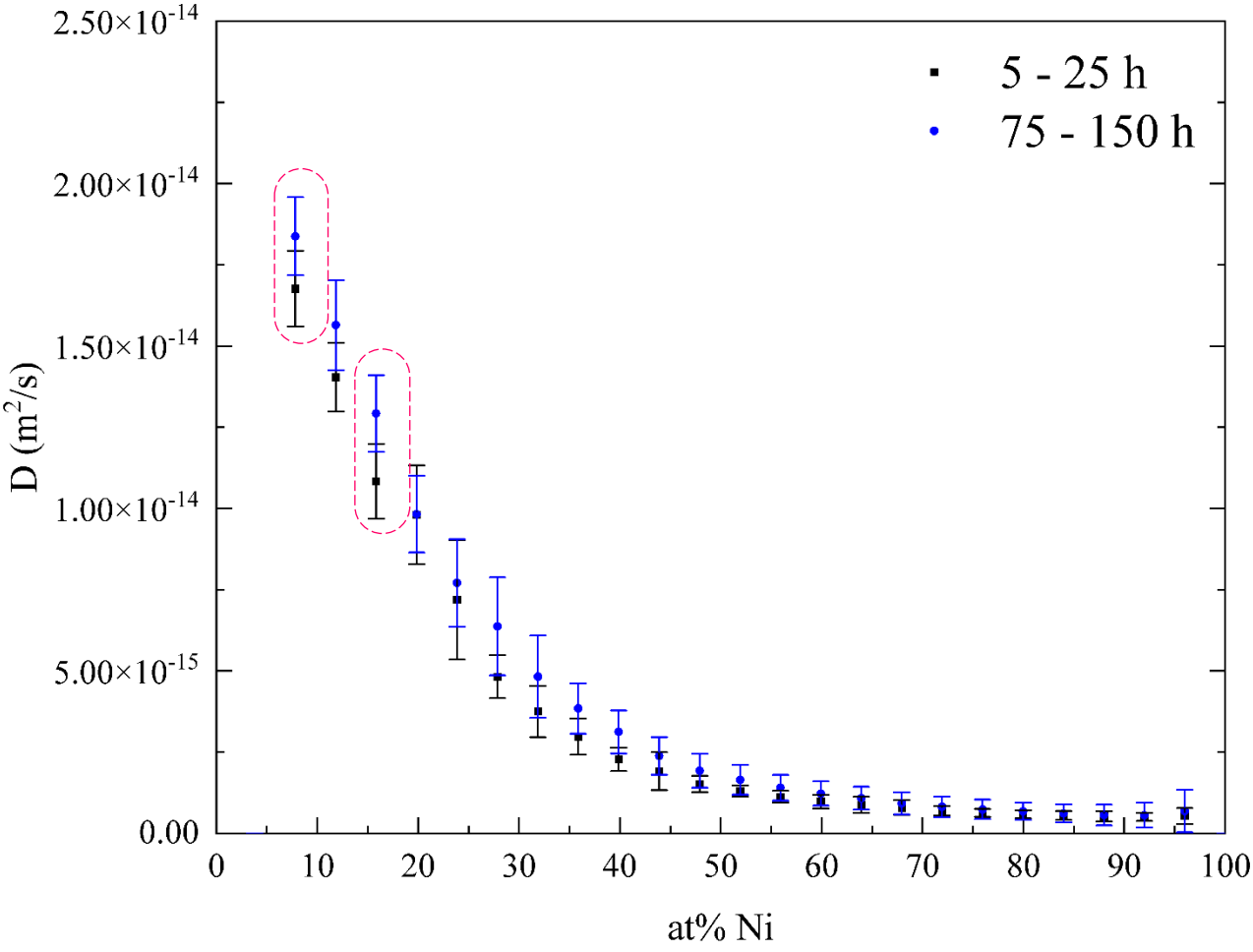

Figure 4.5 – Interdiffusion Coefficients for Cu-Ni System at 950°C for 5-25 h vs. 75-150 h

Table 4.3 – *p*-values of the *t-statistics* for Cu-Ni System at 950°C

Ni at%		7.0	11.0	15.0	19.0	23.0	27.0	31.0
5-25 h vs 25-75 h	p	0.005	0.002	0.001	>>0.2	>>0.2	0.050	0.020
5-25 h vs 75-150 h	p	0.005	0.200	0.020	>>0.2	>>0.2	0.100	0.100
Ni at%	35.0	39.0	43.0	47.0	51.0	55.0	59.0	63.0
5-25 h vs 25-75 h	0.020	0.001	0.010	0.020	0.100	0.200	0.200	>>0.2
5-25 h vs 75-150 h	0.020	0.005	0.200	0.100	0.100	0.200	0.200	>>0.2
Ni at%	67.0 - 95.0							
5-25 h vs 25-75 h 5-25 h vs 75-150 h	>>0.200							

Table 4.4 – Average Interdiffusion Coefficients for Cu-Ni System at 950°C

Time Intervals	25-75 h	Difference in Percentage	5-25 h	Difference in Percentage	75-150 h
$\boldsymbol{D_{Ave}}$	4.9527E-15	+24.49%	3.9783E-15	+15.59%	4.5985E-15
p	–	0.01 - 0.02	–	0.01 - 0.02	–

4.1.3. Verification of Time Effect at 1000°C in Cu-Ni System

In addition to a temperature of 900°C and 950°C, a temperature of 1000°C was also taken into consideration to verify that there is a time effect on the interdiffusion coefficient. The plotted $\widetilde{D}(C)$ curves with error bars that compare shorter and longer diffusion times at 1000°C are shown in *Figures 4.6* and *4.7*. The corresponding *p*-values of the *t-statistics* are listed in *Table 4.5*. A comparison of the D_{Ave} results is provided in *Table 4.6*.

Unlike at 950°C, the $\widetilde{D}(C)$ curves remarkably vary with diffusion time at 1000°C. As shown in *Figures 4.6* and *4.7*, the $\widetilde{D}(C)$ curves with error bars show noticeable variations with diffusion time. The *p*-values of the *t-statistics* in *Table 4.5* statistically validate the reliability of these error bars, especially for 7 at% - 39 at% Ni. This might suggest that variations are more substantial in the Cu-rich interdiffusion region, similar to the phenomenon observed for 900°C. Overall, this tendency in the Cu-rich region has been noticed in 2 out of 3 temperature conditions in the Cu-Ni system. To fully confirm this tendency, more investigations can be done in the future.

Meanwhile, the D_{Ave} results in *Table 4.6* also show noticeable variations with time. The difference in percentage for both compared time intervals is higher than the empirically derived 15%, which ranges from 30% to 50%. Moreover, the time effect on the interdiffusion coefficients shows another potential characteristic for shorter diffusion treatments. That is, the differences are noticeable when a time interval of 5-25 h is compared with the 2 other longer time intervals, while the comparison between the 2 longer intervals shows minor differences.

Thus, both the graphical and statistical results show that the interdiffusion coefficients have a noticeable variation with diffusion time, which suggests that there is a time effect on the interdiffusion coefficients for the Cu-Ni system at 1000°C.

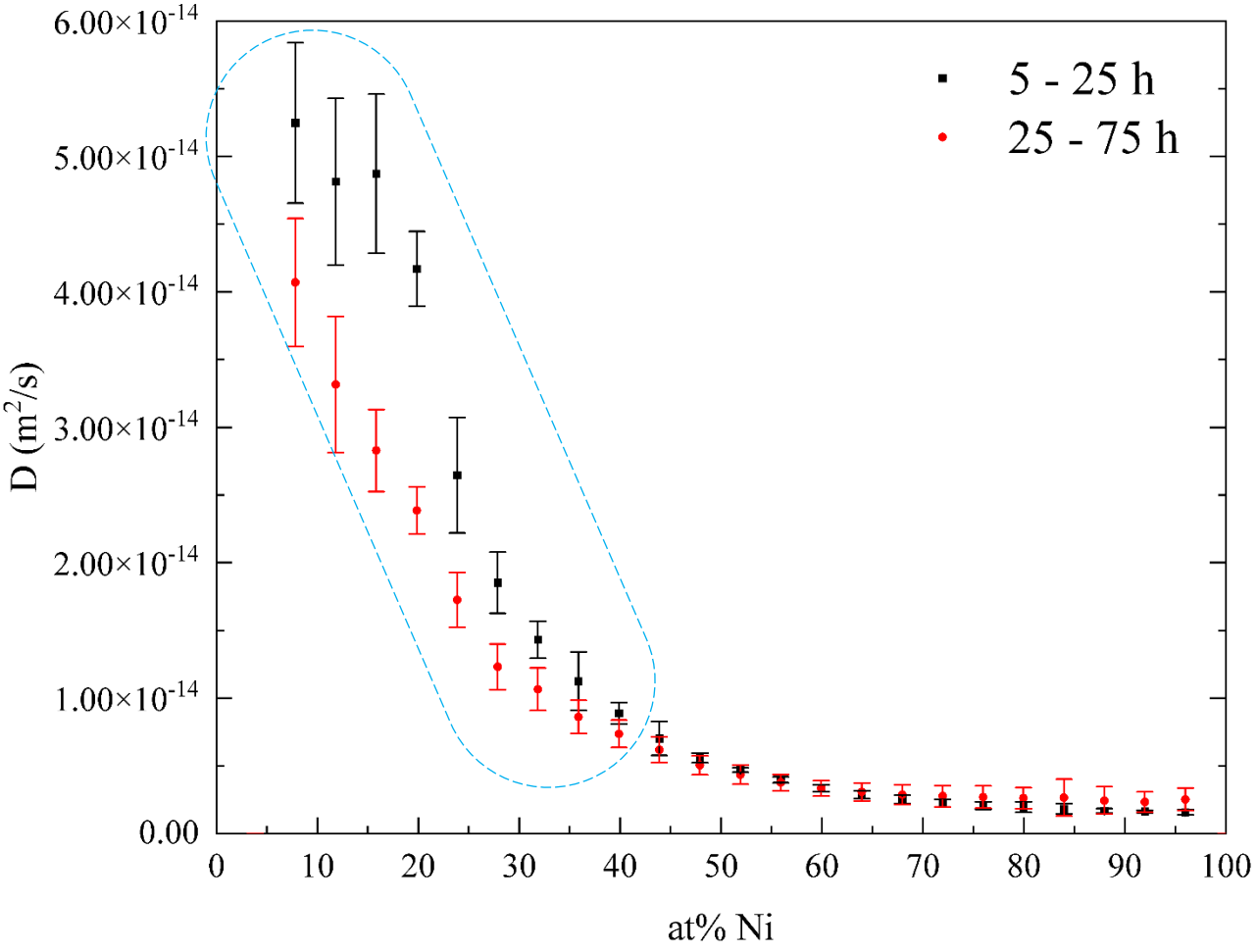

Figure 4.6 – Interdiffusion Coefficients for Cu-Ni System at 1000°C for 5-25 h vs. 25-75 h

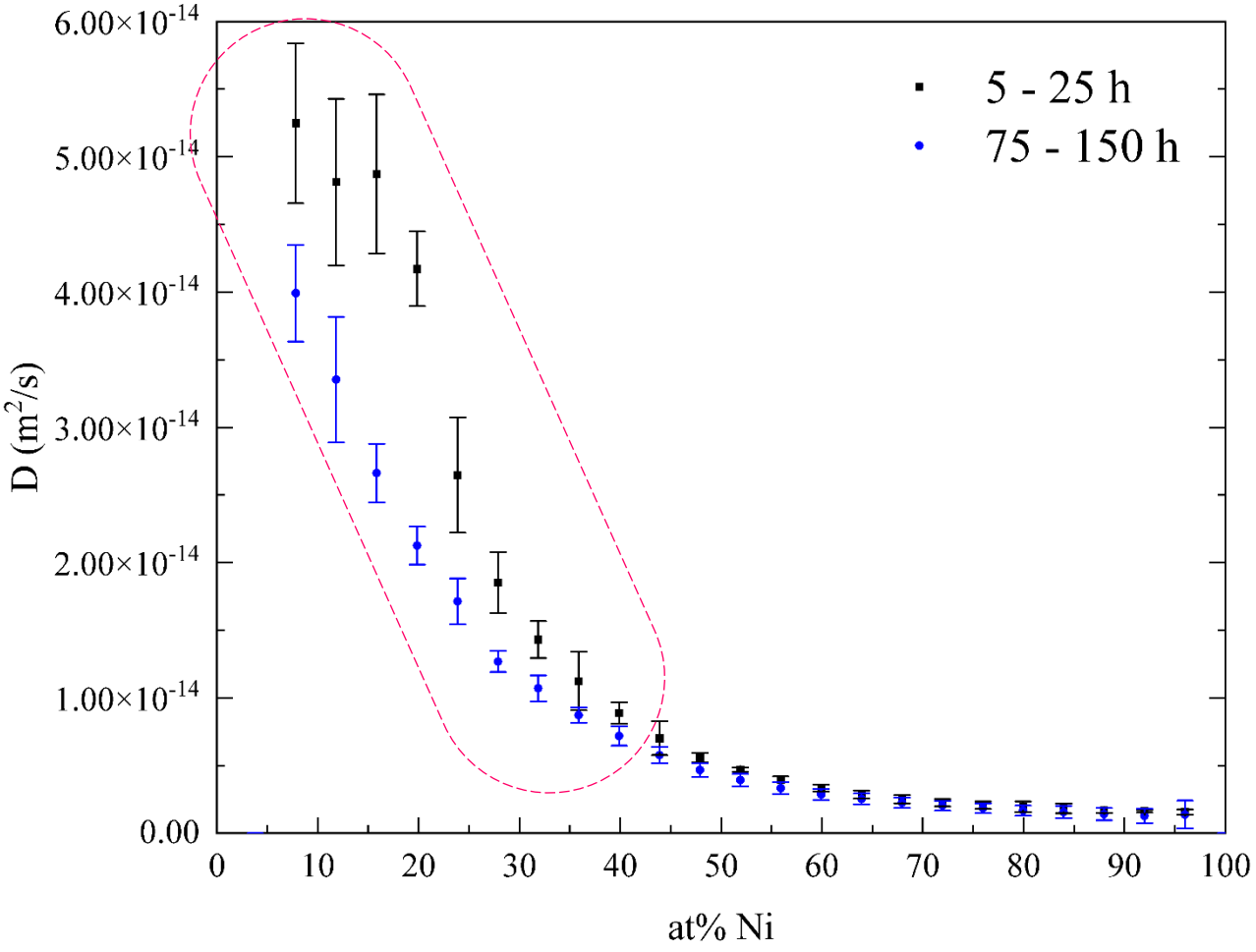

Figure 4.7 – Interdiffusion Coefficients for Cu-Ni System at 1000°C for 5-25 h vs. 75-150 h

Table 4.5 – *p*-values of the *t-statistics* for Cu-Ni System at 1000°C

Ni at%		7.0	11.0	15.0	19.0	23.0	27.0	31.0
5-25 h vs 25-75 h	p	0.001	0.001	0.001	0.001	0.001	0.001	0.001
5-25 h vs 75-150 h	p	0.001	0.001	0.001	0.001	0.001	0.001	0.001
Ni at%	35.0	39.0	43.0	47.0	51.0	55.0	59.0	63.0
5-25 h vs 25-75 h	0.020	0.002	0.200	0.200	>>0.2	>>0.2	>>0.2	>>0.2
5-25 h vs 75-150 h	0.020	0.001	0.050	0.002	0.001	0.002	0.020	0.100
Ni at%	67.0 - 95.0							
5-25 h vs 25-75 h 5-25 h vs 75-150 h	>>0.200							

Table 4.6 – Average Interdiffusion Coefficients for Cu-Ni System at 1000°C

Time Intervals	25-75 h	Difference in Percentage	5-25 h	Difference in Percentage	75-150 h
$\boldsymbol{D_{Ave}}$	1.0715E-14	+36.45%	1.4621E-14	+45.26%	1.0065E-14
p	–	< 0.001	–	< 0.001	–

4.1.4. Summary of Time Effect Verification in Cu-Ni System

In summary, since $\widetilde{D}(C)$ and D_{Ave} vary with diffusion time for all three temperature conditions, the occurrence of a time effect can be experimentally verified for the Cu-Ni system, especially for the temperature range of 900 – 1000°C. Even though the finding contradicts conventional views, the time effect is found multiple times. Apart from this, other aspects of this result set do not contradict traditional thoughts. E.g., the D_{Ave} results are positively correlated with increasing diffusion temperatures for all three diffusion time intervals. Additionally, there are other notable observations of the time effect in this study. For example, the diffusion time has a more profound effect in the Cu-rich interdiffusion regions (as shown in *Figures 4.1 - 4.3*, *4.6* and *4.7*.) and mostly, but not always (e.g., the diffusion treatment at 900°C for 150-450 h is an exception), during the early diffusion times in the Cu-Ni system.

As a result, the conventional recognition that interdiffusion coefficients are independent on diffusion time has to be reconsidered. Thus, the time effect on interdiffusion coefficients in the Cu-Ni system has been validated, and the most suggestive underlying factor for this time effect is subsequently discussed.

4.2. Underlying Factor of Time Effect

Informed by previous studies, the presence of DIS in interdiffusion is a plausible reason for the time effect on interdiffusion coefficients. As previously mentioned, controlling the experimental parameters/conditions can eliminate other possible underlying factors (A and B in Section 2.3.2).

As indicated in related studies [10–21, 28] on DIS, the DIS not only evolves with $\frac{\partial C}{\partial x}$ but also has a noticeable influence back on interdiffusion. This is known as stress-induced diffusion [20], and the complex driving force that influences the interdiffusion process could be the origin [24, 25].

On the other hand, stress-induced interdiffusion can influence DIS as well. Therefore, the schematic diagram (*Figure 2.5* from [11]) can be tailored into *Figure 4.8*.

However, as mentioned previously in Section 2.3.2.3, the direct and real-time measurement of DIS can be particularly challenging due to current technical limitations. Therefore, the direct investigation of DIS is not quite feasible, and an indirect approach needs to be considered. Due to the strong correlation between DIS and the variation in $\frac{\partial C}{\partial x}$, the concentration gradient in space ($\frac{\partial C}{\partial x}$) is a feasible indirect approach.

This is based on the fundamental concept that, with the presence of DIS, for any given temperature and diffusion time period, change in $\frac{\partial C}{\partial x}$ can cause the interdiffusion coefficient to change. However, without DIS, any change in $\frac{\partial C}{\partial x}$ within a specific diffusion time, at a given temperature, would not cause the interdiffusion coefficient to change. Accordingly, if a change in $\frac{\partial C}{\partial x}$ within a given diffusion time period causes the interdiffusion coefficient to isothermally change, then it is an indication that DIS is operative.

To change $\frac{\partial C}{\partial x}$ while keeping the diffusion time and temperature constant, one approach used in the present work is two material conditions: one material is initially free of solute atoms prior to diffusion, and the other is not. The solute atoms it contains can have different distributions, whether uniform or non-uniform, when plotted against the distance in space. Thus, it resulted in having a pre-existing uniform or non-uniform solute distribution prior to the diffusion treatments and accordingly changed the $\frac{\partial C}{\partial x}$. As a result, the focus can be on the influence of $\frac{\partial C}{\partial x}$ on the interdiffusion coefficients in the Cu-Ni system by comparing the diffusion treatments with and without a pre-existing solute distribution.

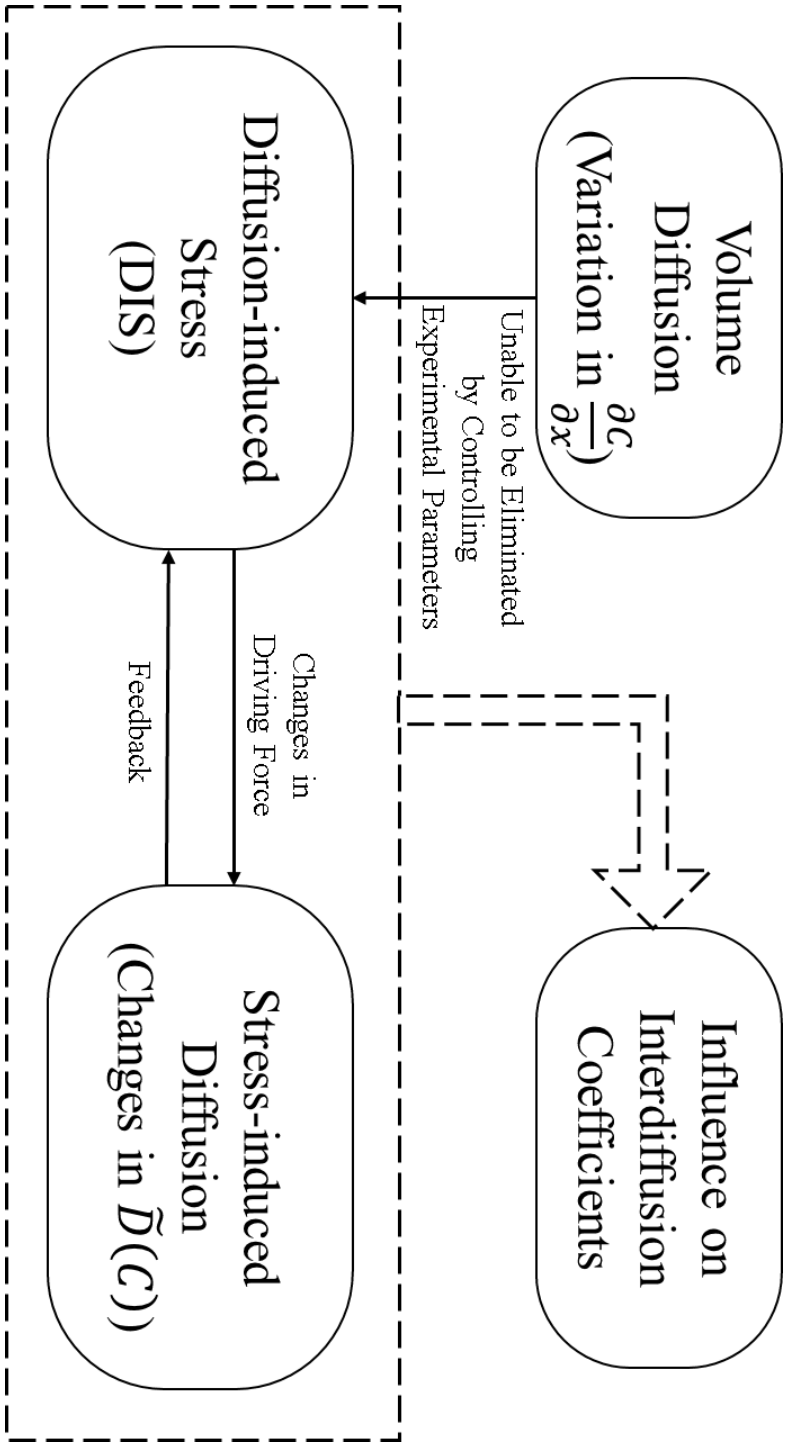

Figure 4.8 – Diffusion-induced Stress and Its Influence on Interdiffusion

4.3. Influence of Pre-existing Uniform Solute Distribution

As previously mentioned in Section 4.2, the variation in $\frac{\partial C}{\partial x}$ can be used as an indirect approach for investigating the influence of DIS on the interdiffusion coefficients. Viz, using the $\frac{\partial C}{\partial x}$ as the "litmus test paper" to check whether DIS is operative.

In general cases, the $\frac{\partial C}{\partial x}$ constantly changes when the interdiffusion proceeds with diffusion time. To eliminate all the other factors, the diffusion time intervals and temperatures are kept constant so that $\frac{\partial C}{\partial x}$ is the only changing variable. Changing the $\frac{\partial C}{\partial x}$ is done by considering a pre-existing solute distribution, and there are two designed ways to do so in this study.

The first means is to replace the pure Cu with $Cu_{90}Ni_{10,}$ which is a Cu-based alloy, and keep the diffusion treatment time intervals constant. This Cu-based alloy has a pre-existing uniform solute distribution with 10 at% Ni on only one side of the diffusion system. In this way, the overall concentration range of Ni has been reduced from 100 at% - 0 at% down to 100 at% - 10 at%. As a result, although the diffusion temperatures and diffusion time intervals are kept constant, the concentration gradient in space ($\frac{\partial C}{\partial x}$) at each concentration point can still be changed. Therefore, an investigation with constant diffusion time can be carried out.

A comparison of a time-constant $\widetilde{D}(C)$ and D_{Ave} between with vs. without a pre-existing uniform solute distribution at different temperature conditions is provided in the following sections. The indicators are still the error bars, differences in percentages and *p*-values of the *t-statistics* with the same benchmarks (e.g., empirically derived benchmark 15%, p<0.05, etc.). The details are provided in the following sections.

4.3.1. Influence of Pre-existing Uniform Solute Distribution at 900°C

In this section, comparisons are made between with and without a pre-existing uniform solute distribution (10 at% Ni) at 900°C. The 5 at% near both dilute ends have been removed due to the limitation of the SF equation at the dilute ends. Since the overall concentration range has been reduced, the comparisons are carried out for 15 at% - 95 at% of Ni.

The $\widetilde{D}(C)$ curves with error bars show apparent differences when the $\frac{\partial C}{\partial x}$ is changed with a pre-existing uniform solute distribution, as shown in *Figures 4.9 - 4.11*. Such significant differences have been found in all three constant time intervals – 5-25 h, 25-75 h, and 75-150 h. The *p*-values shown in *Table 4.8* statistically validate the reliability of error bars. The concentration points with clearly separated error bars also have *p*-values less than 0.05. Meanwhile, observable differences of D_{Ave} for all 3 time conditions can be found in *Table 4.7*. The percentage of the difference for all three is much greater than the 15% empirical benchmark, and they are undoubtedly higher than the range of uncertainty (in *Table 3.3*) for the experimental data in this study.

Therefore, the influence of a changed $\frac{\partial C}{\partial x}$ on the interdiffusion coefficient is quite noticeable at 900°C. Since the $\frac{\partial C}{\partial x}$ represents the DIS, the DIS is highly likely to influence the interdiffusion coefficients. As a result, the DIS could be the most suggestive underlying factor for the interdiffusion coefficient variations at 900°C. Furthermore, this includes the previously verified time effect on the interdiffusion coefficient, since the $\frac{\partial C}{\partial x}$ can undoubtedly change with diffusion time during an isothermal diffusion treatment. Similar to the investigation in Section 4.1, the diffusion treatments with and without a pre-existing uniform solute distribution were carried out at 950°C and 1000°C respectively, to cover more temperature conditions. The details are discussed in the following sections.

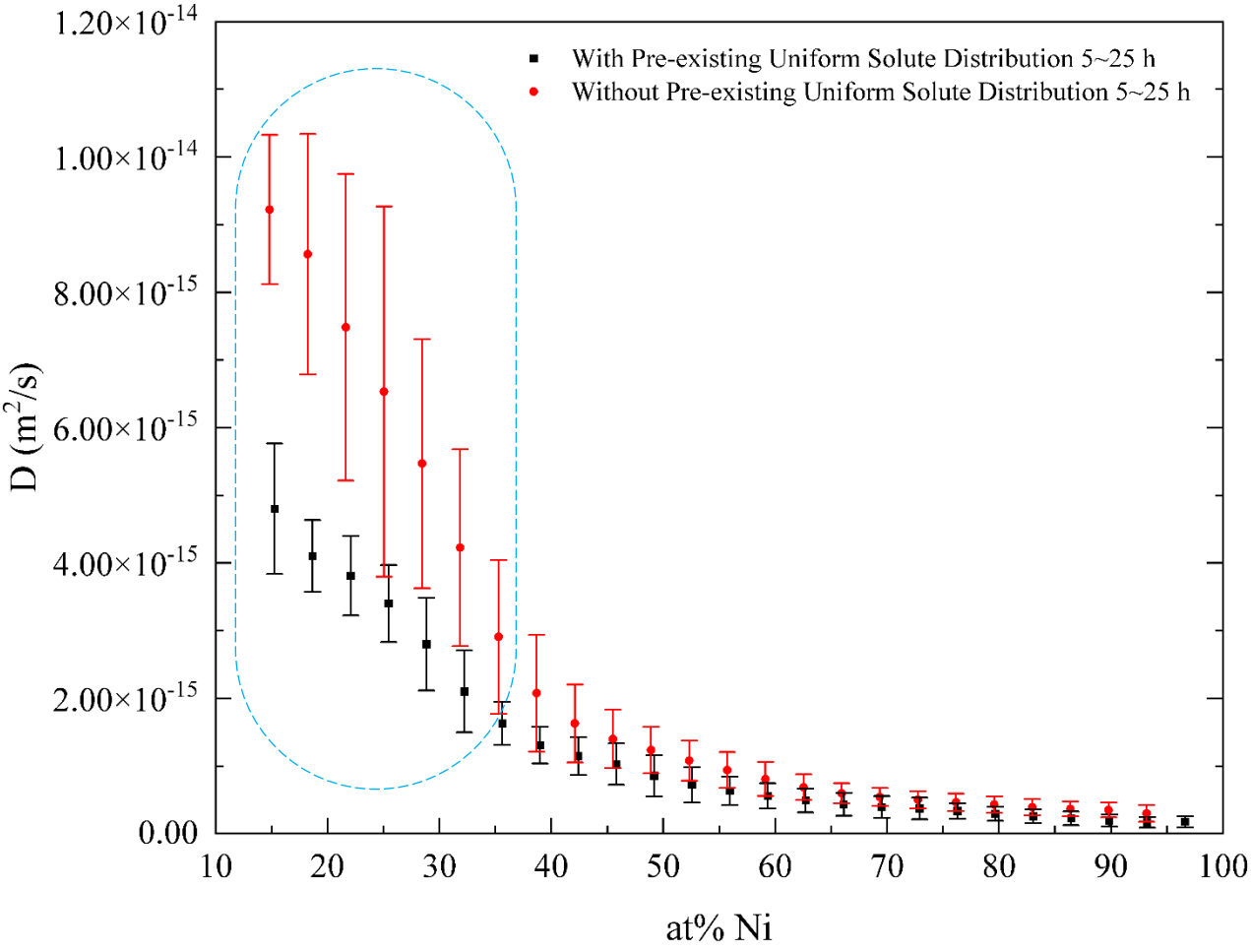

Figure 4.9 – Interdiffusion Coefficients – with vs. without Pre-existing Uniform Solute Distribution at 900°C for 5-25 h

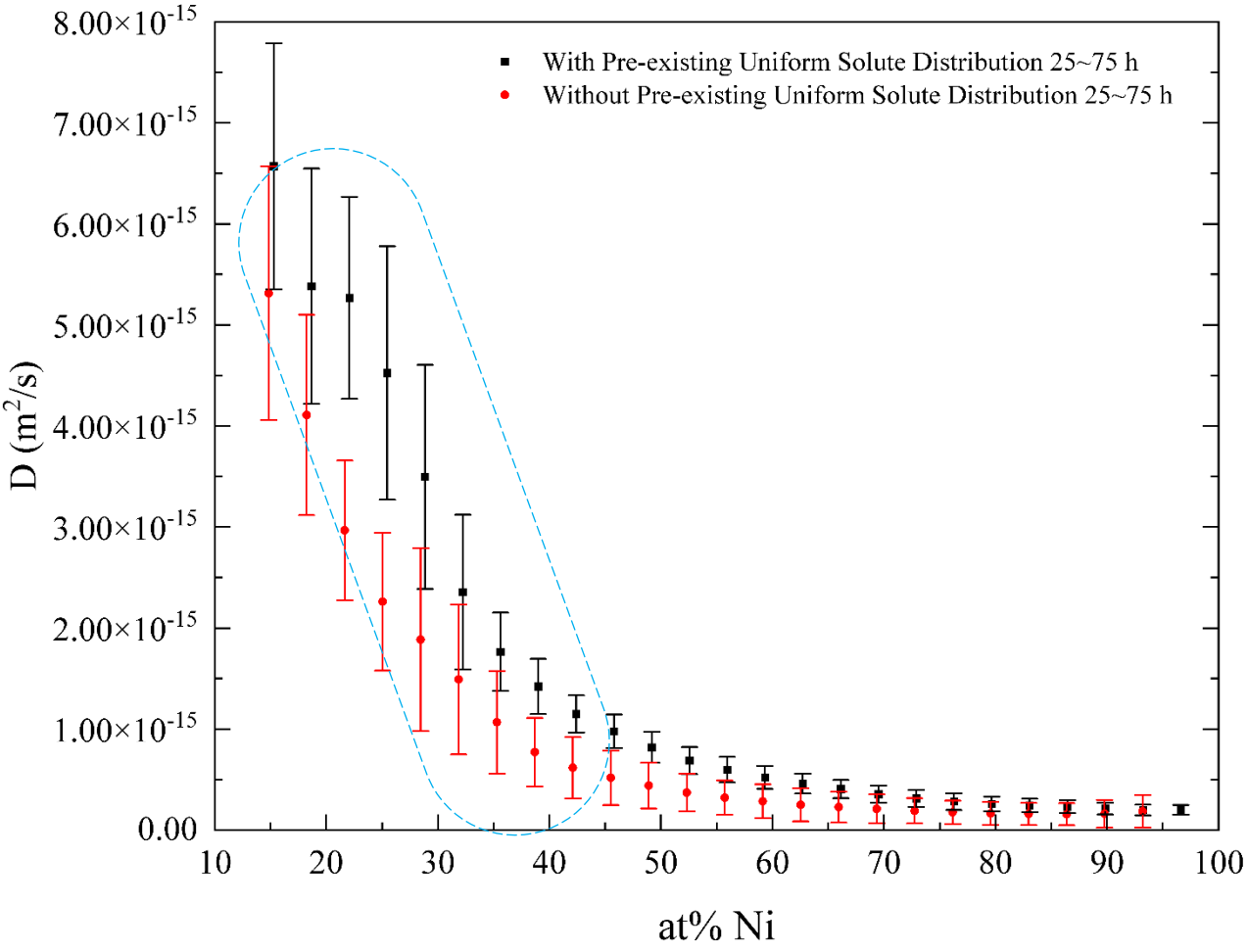

Figure 4.10 – Interdiffusion Coefficients – with vs. without Pre-existing Uniform Solute Distribution at 900°C for 25-75 h

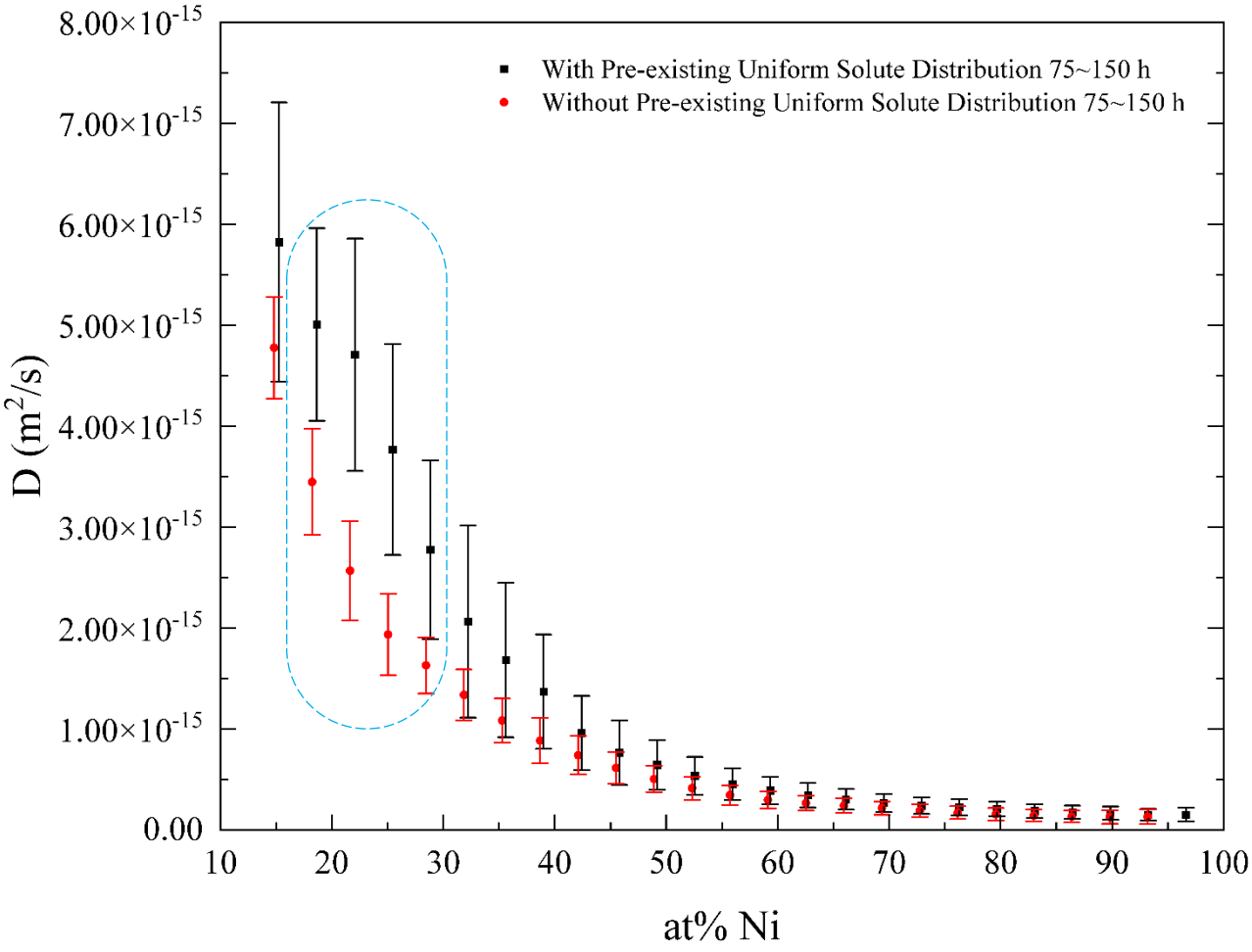

Figure 4.11 – Interdiffusion Coefficients – with vs. without Pre-existing Uniform Solute Distribution at 900°C for 75-150 h

Table 4.7 – Average Interdiffusion Coefficients – with vs. without Pre-existing Uniform Solute Distribution at 900°C

900°C (15-95 at%)	$D_{Ave,Pure}$ (m^2/s)	Difference in Percentage	$D_{Ave,Alloy}$ (m^2/s)
5-25 h	2.2900E-15	✓ 78.49% (p=0.002 - 0.005)	1.2830E-15
25-75 h	9.2700E-16	✓ 63.74% (p=0.005 - 0.01)	1.5178E-15
75-150 h	8.5600E-16	✓ 53.01% (p=0.01 - 0.02)	1.3098E-15

Table 4.8 – *p*-values of the *t-statistics* – with vs. without Pre-existing Uniform Solute Distribution at 900°C

Ni at%		20.2	23.6	27.0	30.4	33.8	37.2	40.6
5-25 h	p	0.001	0.001	0.001	0.010	0.001	0.010	0.020
25-75 h	p	0.050	0.002	0.001	0.001	0.020	0.020	0.001
75-150 h	p	0.020	0.001	0.001	0.001	0.050	0.100	0.100
Ni at%	44.0	47.4	50.8	54.2	57.6	61.0	64.4	67.8
5-25 h	0.100	0.200	0.100	0.050	0.050	0.100	0.100	0.100
25-75 h	0.001	0.001	0.001	0.001	0.002	0.005	0.010	0.020
75-150 h	0.200	>>0.2	>>0.2	0.200	0.200	0.200	0.200	>>0.2
Ni at%	71.2 - 95.0							
5-25 h	>>0.050 (No Noticeable Difference)							
25-75 h								
75-150 h								

4.3.2. Influence of Pre-existing Uniform Solute Distribution at 950°C

Comparisons made between with and without a pre-existing uniform solute distribution at 950°C are presented in this section. The $\widetilde{D}(C)$ curves with error bars are shown in *Figures 4.12* and *4.13*. *Table 4.9* presents the D_{Ave} results and differences in percentage, while the *p*-values of the *t-statistics* are listed in *Table 4.10*.

Unlike the results at 900°C, the variation of D_{Ave} at 950°C for the time interval of 25-75 h is not very noticeable. Meanwhile, the $\widetilde{D}(C)$ curves with error bars only show noticeable differences at 23.6 at% and 27.0 at%. Similarly, the variation of D_{Ave} for the time interval of 5-25 h is not apparent either, with a minor change in the $\widetilde{D}(C)$ curves with error bars or in their *p*-values. Therefore, the data are not plotted.

The maximum difference among the average interdiffusion coefficients (approximately 18.75%) can be found in the results for the time interval of 75-150 h. The statistical indicator *p*-value shows that the difference in percentage exceeds the benchmark ($p < 0.05$). Correspondingly, concentration points such as 23.6 at% - 30.4 at% in the $\widetilde{D}(C)$ curves have noticeable differences according to both the error bars and *p*-values. Moreover, all of these differences are more observable in the Cu-rich region (when Cu at% > Ni at%).

Overall, a pre-existing uniform solute distribution can still influence the interdiffusion coefficients to some extent at 950°C in the Cu-Ni system, even though it is not as apparent as the case at 900°C. Subsequently, comparisons at 1000°C are presented in the next section to determine whether such influence is applicable at 1000°C.

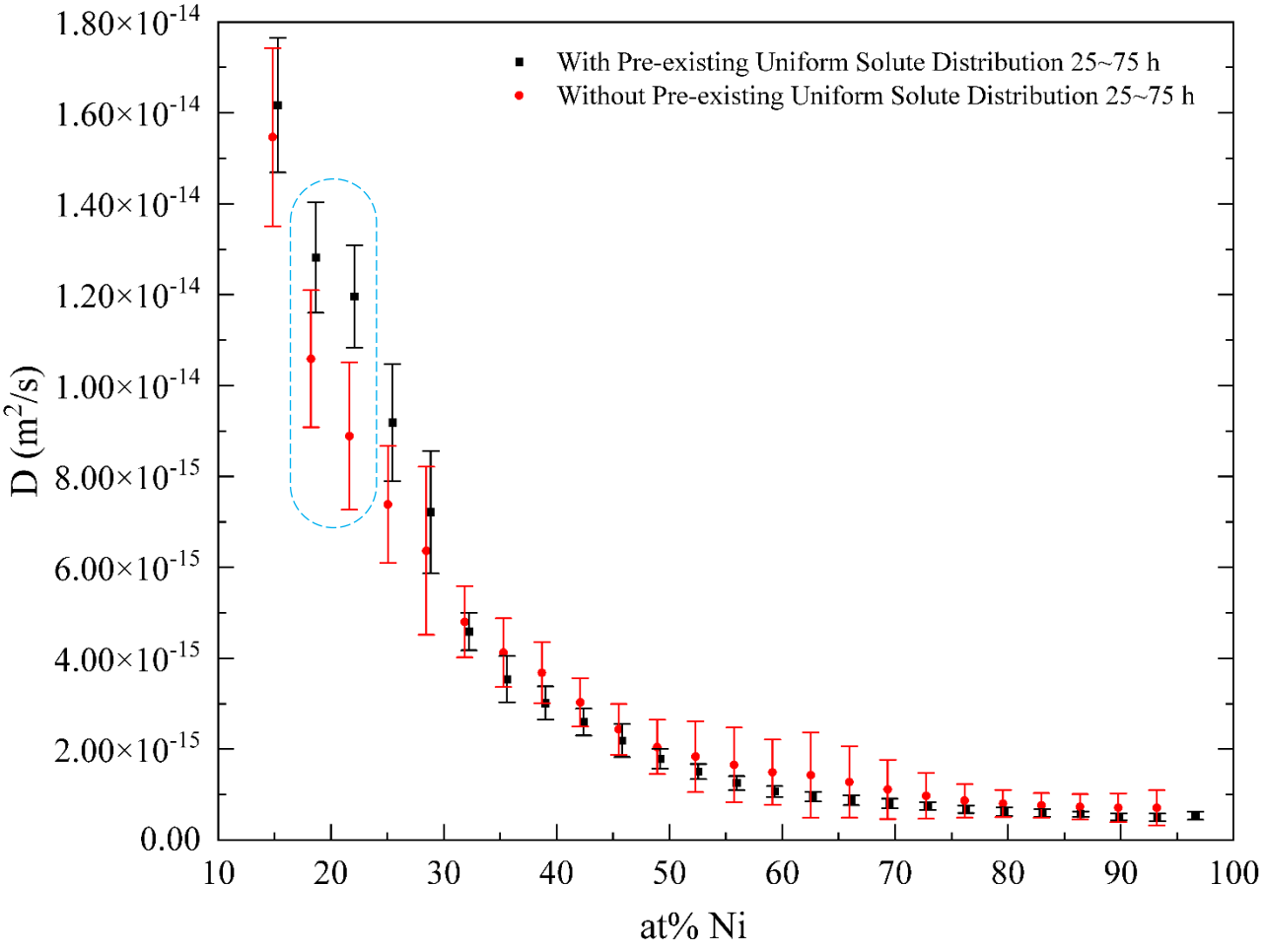

Figure 4.12 – Interdiffusion Coefficients – with vs. without Pre-existing Uniform Solute Distribution at 950°C for 25-75 h

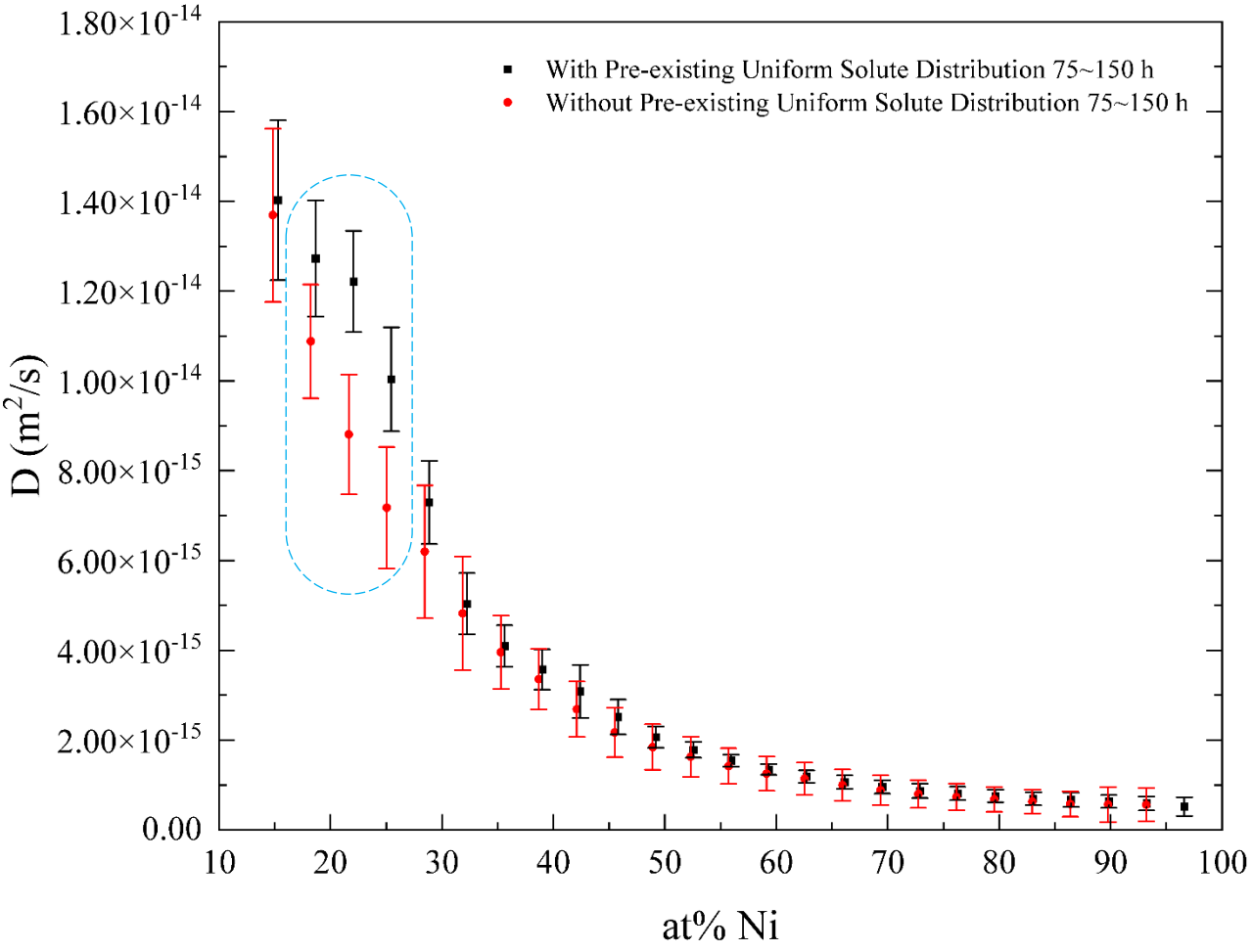

Figure 4.13 – Interdiffusion Coefficients – with vs. without Pre-existing Uniform Solute Distribution at 950°C for 75-150 h

Table 4.9 – Average Interdiffusion Coefficients – with vs. without Pre-existing Uniform Solute Distribution at 950°C

950°C (15-95 at%)	$D_{Ave,Pure}$ (m^2/s)	Difference in Percentage	$D_{Ave,Alloy}$ (m^2/s)
5-25 h	2.5737E-15	9.03% (p>0.2)	2.8061E-15
25-75 h	3.2183E-15	4.54% (p>0.2)	3.3645E-15
75-150 h	3.0173E-15	18.75% (p=0.05 - 0.02)	3.5831E-15

Table 4.10 – *p*-values of the *t-statistics* – with vs. without Pre-existing Uniform Solute Distribution at 950°C

Ni at%		20.2	23.6	27.0	30.4	33.8	37.2	40.6
5-25 h	p	>>0.2	>>0.2	0.100	0.050	>>0.2	>>0.2	>>0.2
25-75 h	p	0.200	0.001	0.001	0.200	>>0.2	>>0.2	0.100
75-150 h	p	>>0.2	0.002	0.001	0.020	>>0.2	>>0.2	>>0.2

Ni at%	44.0 - 95.0
5-25 h	>>0.050 (No Noticeable Difference)
25-75 h	
75-150 h	

4.3.3. Influence of Pre-existing Uniform Solute Distribution at 1000°C

Finally, comparisons are made between with and without pre-existing uniform solute distribution (10 at% Ni) at 1000°C. All the control groups (without pre-existing uniform solute distribution) for 900°C, 950°C and 1000°C share the data in Section 4.1.

Comparisons of the $\widetilde{D}(C)$ curves with error bars at 1000°C are shown in *Figures 4.14* and *4.15*. Distinct differences in the interdiffusion coefficients due to variation in the concentration gradient can be found for time intervals of 5-25 h and 75-150 h. Meanwhile, the *p*-values in *Table 4.12* statistically validate the reliability of these differences. Based on the shape of the $\widetilde{D}(C)$ curves, again, there is a profound effect in the regions that are Cu-rich. Since the diffusion time intervals are kept constant in this case, the tendency in shorter diffusion treatment is not applicable here.

Corresponding to the differences in the interdiffusion coefficients from the $\widetilde{D}(C)$ curves, the D_{Ave} results show noticeable differences for time intervals of 5-25 h and 75-150 h as well. *Table 4.11* shows that both differences in percentage are within the range of 25 - 65%, which is significantly higher than the empirical benchmark of 15%. The only time interval that shows a minor difference is 25-75 h, while both the $\widetilde{D}(C)$ curves with error bars and D_{Ave} results are nearly the same.

Overall, the changed $\frac{\partial C}{\partial x}$ once again can profoundly influence the interdiffusion coefficients at 1000°C in the Cu-Ni system. Therefore, the one that $\frac{\partial C}{\partial x}$ represents could be the most suggestive underlying factor of interdiffusion coefficient variations at 1000°C.

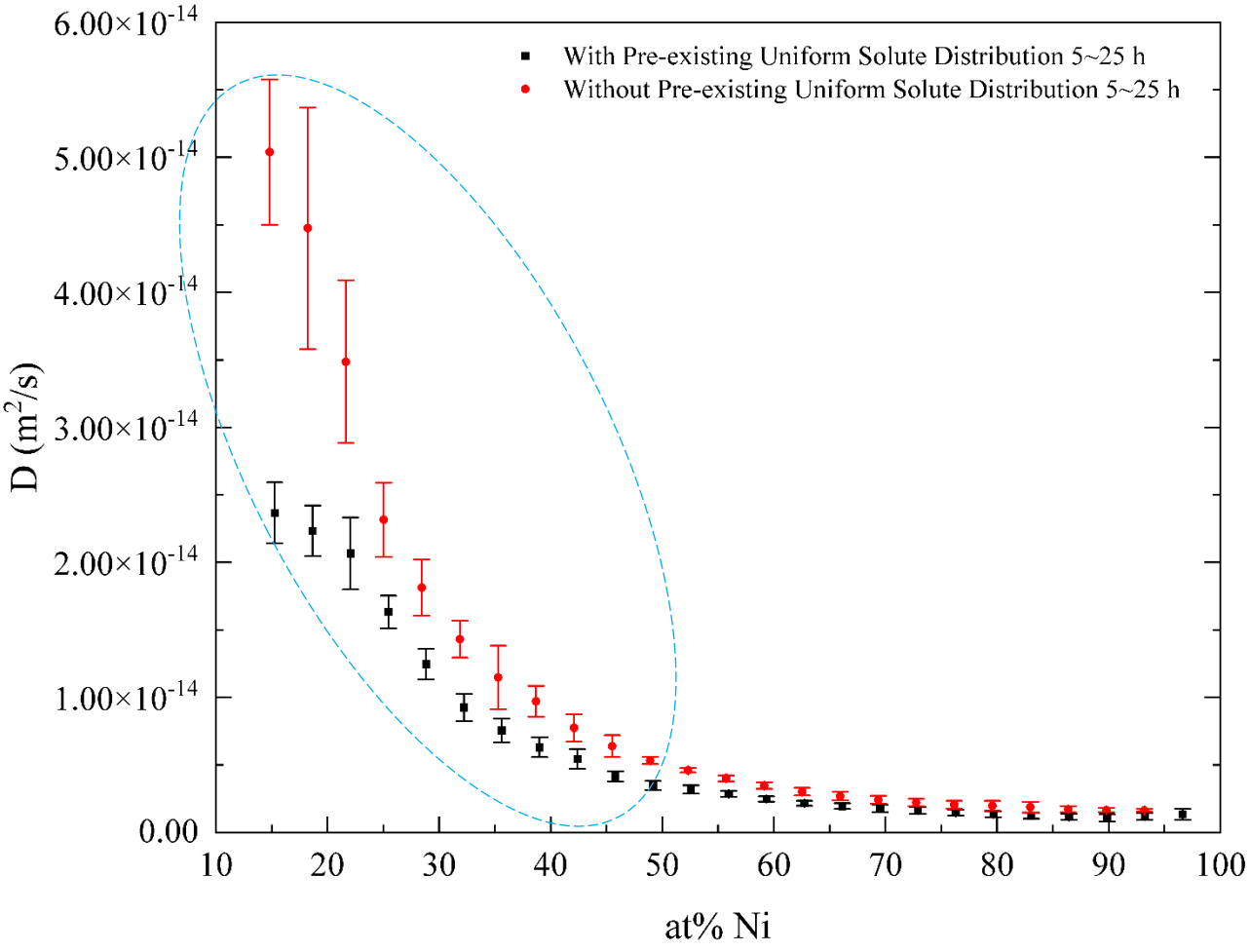

Figure 4.14 – Interdiffusion Coefficients – with vs. without Pre-existing Uniform Solute Distribution at 1000°C for 5-25 h

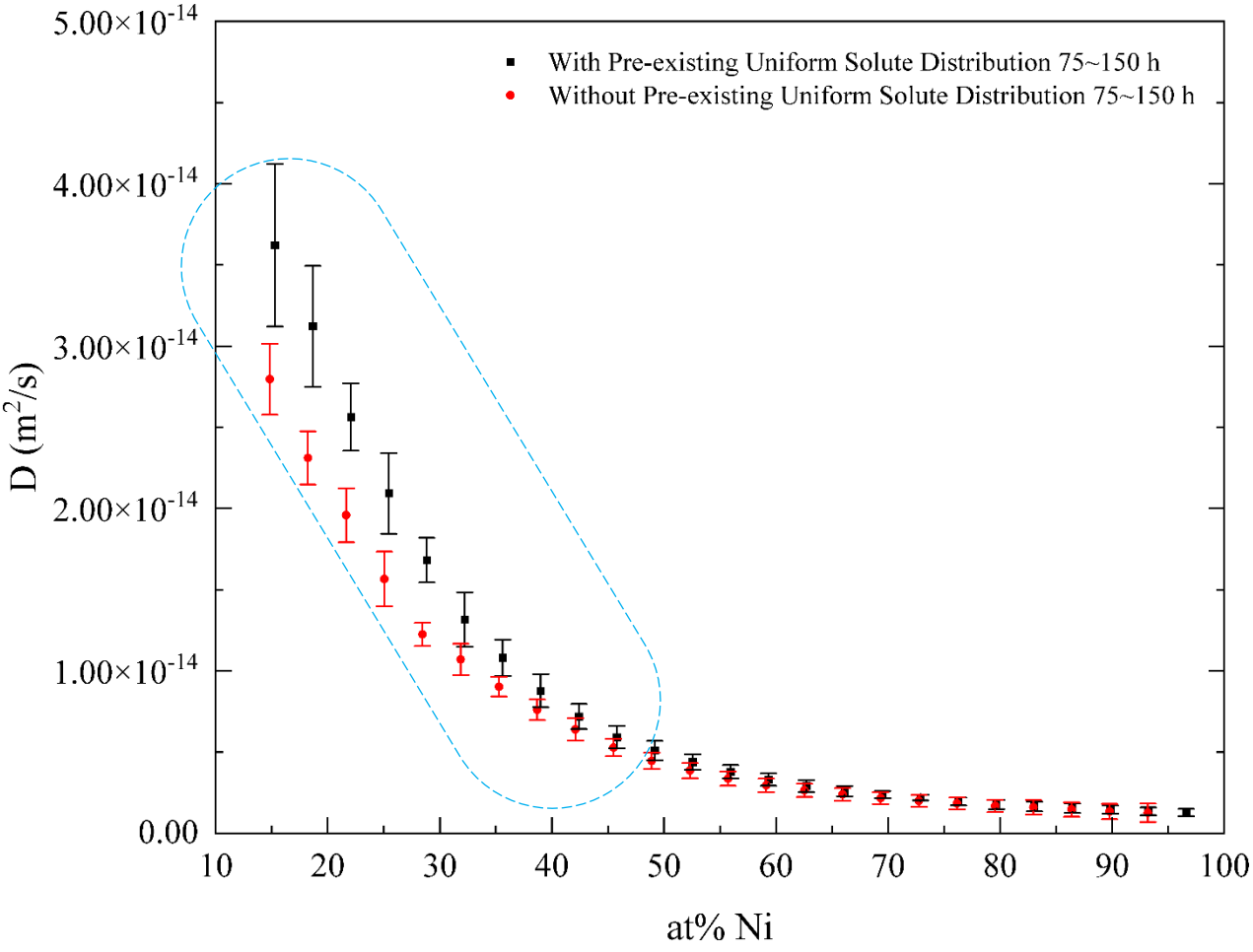

Figure 4.15 – Interdiffusion Coefficients – with vs. without Pre-existing Uniform Solute Distribution at 1000°C for 75-150 h

Table 4.11 – Average Interdiffusion Coefficients – with vs. without Pre-existing Uniform Solute Distribution at 1000°C

1000°C (15-95 at%)	$D_{Ave,Pure}$ (m^2/s)	Difference in Percentage	$D_{Ave,Alloy}$ (m^2/s)
5-25 h	1.0025E-14	✓ 61.95% (p<0.001)	6.1902E-15
25-75 h	7.3315E-15	1.47% (p>0.2)	7.2256E-15
75-150 h	6.6908E-15	✓ 26.20% (p=0.001-0.002)	8.4436E-15

Table 4.12 – *p*-values of the *t-statistics* – with vs. without Pre-existing Uniform Solute Distribution at 1000°C

Ni at%		20.2	23.6	27.0	30.4	33.8	37.2	40.6
5-25 h	p	0.001	0.001	0.001	0.001	0.001	0.001	0.001
25-75 h	p	>>0.2	>>0.2	0.050	0.005	>>0.2	>>0.2	>>0.2
75-150 h	p	0.002	0.001	0.001	0.001	0.001	0.001	0.005
Ni at%	44.0	47.4	50.8	54.2	57.6	61.0	64.4	67.8
5-25 h	0.001	0.001	0.001	0.001	0.001	0.001	0.001	0.001
25-75 h	>>0.2	0.200	>>0.2	>>0.2	>>0.2	>>0.2	>>0.2	>>0.2
75-150 h	0.050	0.050	0.050	0.050	0.100	0.200	>>0.2	>>0.2
Ni at%	71.2	74.6	78.0	81.4	84.8	88.2	91.6	95.0
5-25 h	0.001	0.001	0.001	0.002	0.001	0.001	0.001	0.100
25-75 h	>>0.2	>>0.2	0.100	0.050	0.100	0.050	0.050	0.020
75-150 h	0.200	>>0.2	>>0.2	>>0.2	>>0.2	>>0.2	>>0.2	>>0.2

4.3.4. Summary of Influence of Pre-existing Uniform Solute Distribution

Overall, when $\frac{\partial C}{\partial x}$ is changed by including a pre-existing uniform solute distribution (10 at% Ni) and keeping diffusion time constant, the profound influence of changes in $\frac{\partial C}{\partial x}$ on the interdiffusion coefficients has been found for all three diffusion temperature conditions.

Due to the previously mentioned strong correlation between DIS and a changing $\frac{\partial C}{\partial x}$, the change in the interdiffusion coefficients, which is caused mainly by changing $\frac{\partial C}{\partial x}$ in the Cu-Ni system is attributable to DIS. According to general acknowledgement, the $\frac{\partial C}{\partial x}$ also changes with diffusion time, the isothermal variation of the interdiffusion coefficient with time in the Cu-Ni system is likewise attributable to DIS.

Additionally, as shown in *Figures 4.9 - 4.11, 4.14* and *4.15*, the influence on the interdiffusion coefficients seems to be more noticeable in the Cu-rich region, which points to the potential of a profound effect in the regions that are Cu-rich. Thus, more investigation can be done to fully confirm this potential characteristic in the future.

Furthermore, as stated in Section 4.3, there are two design approaches to provide the pre-existing solute distribution to carry out a more comprehensive investigation. Apart from the uniform pre-existing solute distribution provided by replacing pure Cu with Cu-based alloy, another approach used in this research is the use of the non-uniform pre-existing solute distribution, which is provided by using a 2-stage diffusion treatment. Therefore, subsequently, the detailed discussions are outlined in the following sections.

4.4. Influence of Pre-existing Non-uniform Solute Distribution

The second approach is designed to provide pre-existing non-uniform solute distribution by performing **2-stage** diffusion treatments in the Cu-Ni system. As the terminology suggests, these diffusion treatments have two stages. The first/initial stage aims to provide a pre-existing non-uniform solute distribution, which will not be included during the analysis of interdiffusion coefficients. Meanwhile, the second/final stage of diffusion treatment should be analyzed.

There are two types of the initial/first stage of heat treatment. A "Pre-existing Non-uniform Solute Distribution Type A" is obtained by performing the initial stage at 900°C for 5 h. A "Pre-existing Non-Uniform Solute Distribution Type B" is obtained by performing the initial stage at 1000°C for 5 h. Then, the second/ final stage consists of diffusion treatments at 950°C for 5 h, 25 h, 75 h, and 150 h. The control groups are the "1-stage or single-stage" diffusion treatments at 950°C, as stated in Section 4.1.2. The diffusion temperature and time are constant; the only difference is whether a pre-existing solute distribution is included.

In this way, the concentration gradients in the second/final stage of diffusion treatments are changed compared to "1-stage or single-stage" diffusion treatments within the same time intervals. Correspondingly, the interdiffusion coefficient comparisons are carried out between with and without a pre-existing non-uniform solute distribution. This is so that the influence on the interdiffusion coefficients can be examined. The results are shown in the following sections. These two pre-existing non-uniform solute distributions are abbreviated to "Type A" and "Type B" for convenience in some cases.

4.4.1. Influence of Pre-existing Non-uniform Solute Distribution Type A

It has been observed that the concentration gradient ($\frac{\partial C}{\partial x}$) variation induced by pre-existing solute distribution becomes insignificant when the diffusion time is longer. As shown in *Figures 4.16 (a), 4.16 (b), 4.16 (c),* when the diffusion time for the second/final stage is 150 h, the variation in $\frac{\partial C}{\partial x}$ is minimal. On the contrary, when the diffusion time is 0 h, the variation in $\frac{\partial C}{\partial x}$ is significant. Therefore, the additional comparisons for the results of 0 - 5 h of diffusion time were carried out.

The comparisons of the $\widetilde{D}(C)$ result for with and without Type A are shown in *Figure 4.17* when the diffusion time is kept constant. The *p*-values of the *t-statistics* are shown in *Table 4.14*, and comparisons of the D_{Ave} result comparisons are presented in *Table 4.13*. Unlike the observed interdiffusion coefficient variations in previous chapters, the overall degree of variation of the interdiffusion coefficient in plotted $\widetilde{D}(C)$ curves caused by a pre-existing non-uniform solute distribution is less obvious.

The $\widetilde{D}(C)$ curves with error bars for 0 - 5 h show noticeable differences for a small concentration range (7 - 27 at% Ni). The corresponding *p*-values validate the reliability. Meanwhile, the D_{Ave} results for both 0 - 5 h and 5 - 25 h have sufficient variations (25% - 30%). Even though the difference of D_{Ave} is 15.17% (slightly higher than the empirical benchmark of 15%) for 75-150 h, the error bars and p-values do not show noticeable variations. Since the average interdiffusion coefficient only serves as an auxiliary indicator, the $\widetilde{D}(C)$ curves with graphical (error bars) and statistical (*p*-values) shall take precedence.

Overall, Type A can effectively influence the interdiffusion coefficient. The results of Type B are discussed in the next section to provide more comprehensive experimental support.

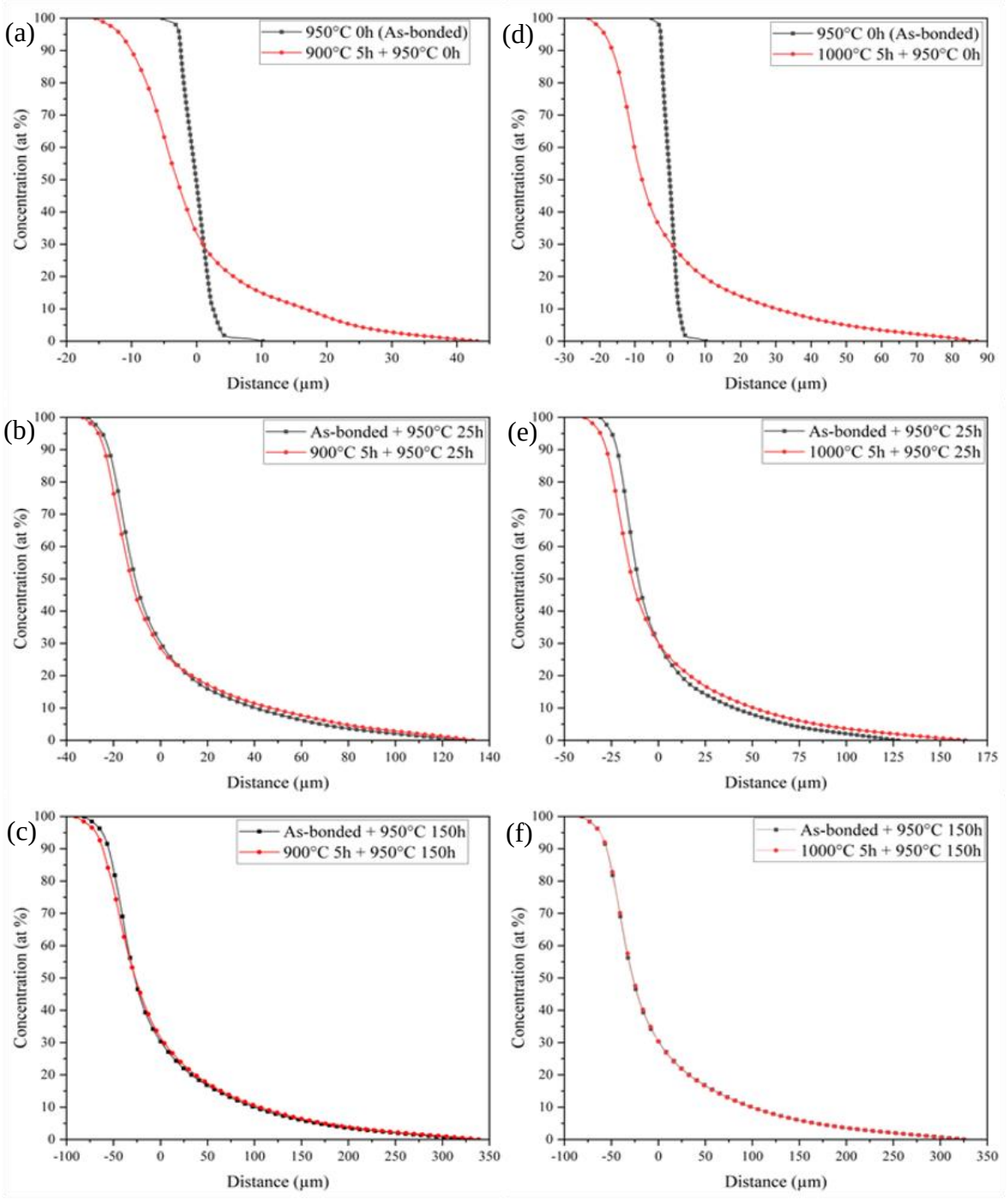

Figure 4.16 – With vs. Without Pre-existing Non-uniform Solute Distribution Type A with (a) 950°C for 0 h, (b) 25 h, (c) 150 h and Type B with (d) 950°C 0 h, (e) 25 h and (f) 150 h

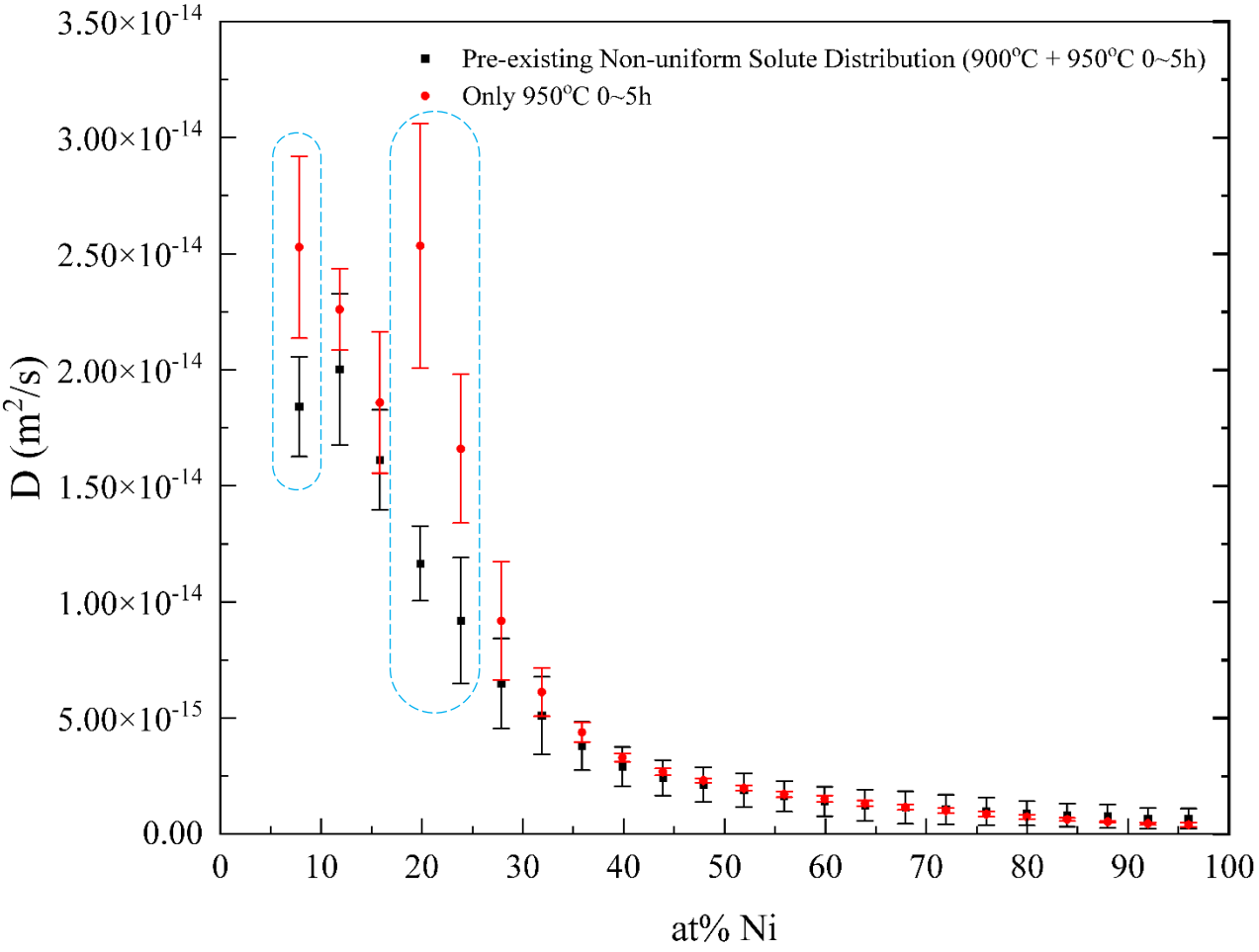

Figure 4.17 – Interdiffusion Coefficients for Cu-Ni system at 950°C for 0-5 h with vs. without a Pre-existing Non-uniform Solute Distribution A

Table 4.13 – Variation due to Pre-existing Non-uniform Solute Distribution Type A

D_{Ave}	Single-stage at 950°C	Difference in Percentage	With Type A at 950°C
0-5 h	6.7749E-15	30.42% (p = 0.001-0.002) ✓✓	5.1944E-15
5-25 h	3.9783E-15	25.15% (p = 0.002 - 0.005) ✓✓	4.9786E-15
25-75 h	4.9527E-15	0.98% (p > 0.2)	4.9048E-15
75-150 h	4.5985E-15	15.17% (p = 0.001 - 0.002)	5.2960E-15

Table 4.14 – *p*-values of the *t-statistics* for Cu-Ni System at 950°C – with vs. without Pre-existing Non-uniform Solute Distribution Type A

Ni at%		7.0	11.0	15.0	19.0	23.0	27.0	31.0
0-5 h	p	<0.050	<0.050	0.100	<0.001	<0.001	0.100	0.200
5-25 h	p	0.001	0.001	0.001	0.010	0.010	0.010	0.200
25-75 h	p	>>0.2	>>0.2	>>0.2	0.020	0.200	>>0.2	>>0.2
75-150 h	p	>>0.2	>>0.2	>>0.2	0.050	0.050	0.200	0.200
Ni at%		35.0 - 95.0						
0-5 h		>>0.050 (No Noticeable Difference)						
5-25 h								
25-75 h								
75-150 h								

4.4.2. Influence of Pre-existing Non-uniform Solute Distribution Type B

The interdiffusion coefficient comparisons for with and without pre-existing non-uniform solute distribution Type B are presented in this section. The diffusion couples were subjected to an initial heat treatment at 1000°C for 5 h before following diffusion treatments at 950°C for 5 h, 25 h, 75 h, and 150 h.

The concentration profile outcomes are shown in *Figures 4.16 (d), 4.16 (e),* and *4.16 (f)*. The variations in $\frac{\partial C}{\partial x}$ due to Type B become negligible when the diffusion time is longer. The concentration profiles for 75 h and 150 h have negligible differences when those for 0 h, 5 h and 25 h are considerably altered due to Type B. The $\widetilde{D}(C)$ curves with error bars have noticeable variations with changing $\frac{\partial C}{\partial x}$ for a time interval of 0-5 h, as shown in *Figure 4.18.* The *p*-values in *Table 4.16* also validate the reliability of these graphical indicators, especially for 7 at% - 31 at% Ni. Corresponding to the $\widetilde{D}(C)$ curves, the D_{Ave} results in *Table 4.15* also show sufficient variations with almost a 100% increase.

Meanwhile, the difference of the D_{Ave} results (*Table 4.15*) for time intervals of 5-25 h and 75-150 h is also higher than the empirical benchmark of 15%. However, the comparison of D_{Ave} can only serve as an auxiliary indicator. Moreover, by plotting the $\widetilde{D}(C)$ curves with error bars, the differences in interdiffusion coefficients are not as evident as for the time interval of 0-5 h. Even though the *p*-values listed in *Table 4.16* also validate the reliability of these differences, the overall differences are not as considerable. Thus, only $\widetilde{D}(C)$ curves with error bars for 0-5 h are plotted.

Overall, Type B can also effectively influence the interdiffusion coefficient. Similar to the results of Type A, the comparison with a time interval of 0-5 h is more worthy of attention. The influence of Types A and B on the interdiffusion coefficient is summarized in the next section.

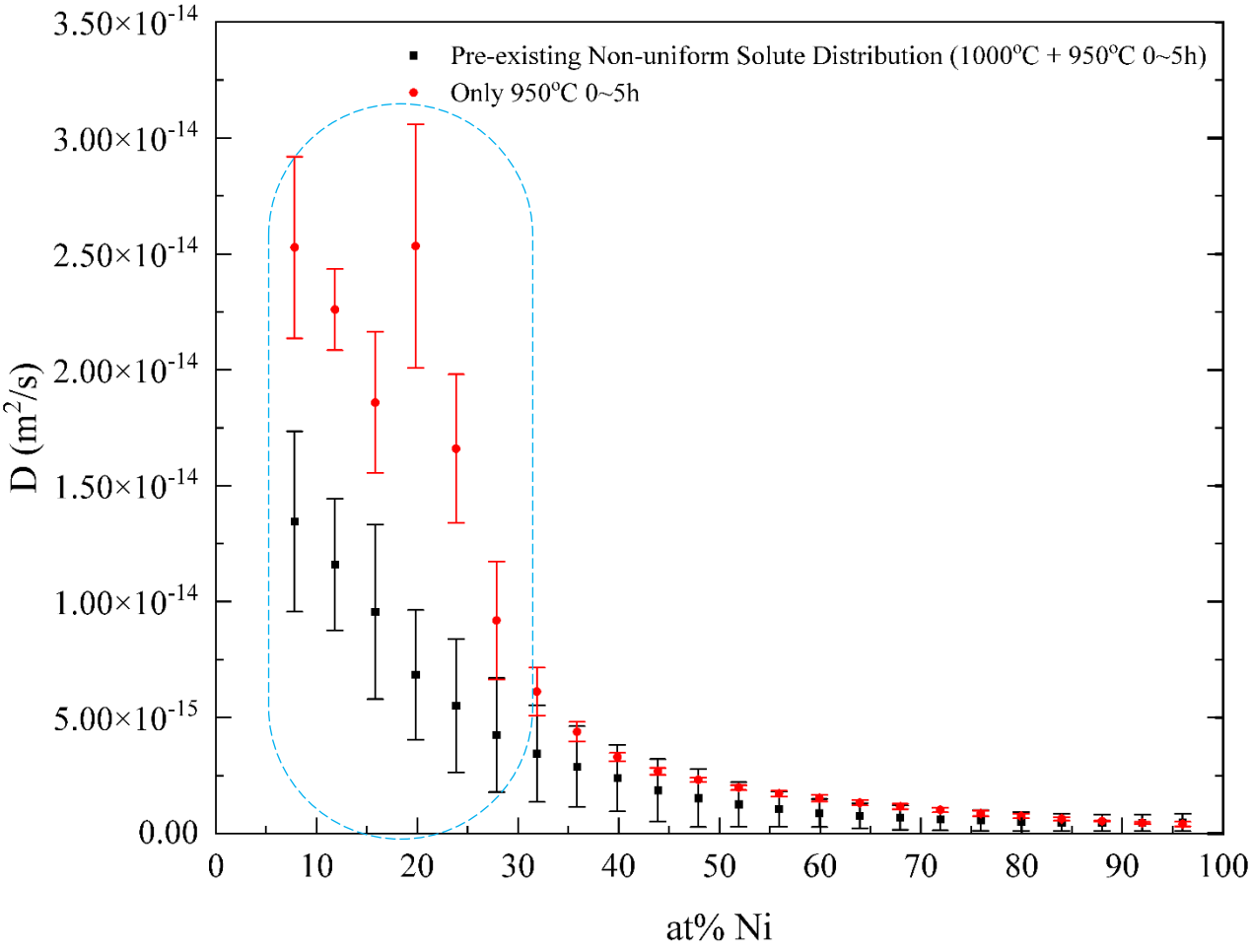

Figure 4.18 – Interdiffusion Coefficients for Cu-Ni system at 950°C for 0-5 h with vs. without Pre-existing Non-uniform Solute Distribution Type B

Table 4.15 – Variation due to Pre-existing Non-uniform Solute Distribution Type B

D_{Ave}	Single-Stage at 950°C	Difference in Percentage	With Type B at 950°C
0-5 h	6.7749E-15	99.73% ($p < 0.001$) ✓✓	3.3919E-15
5-25 h	3.9783E-15	26.13% ($p = 0.002$ - 0.005) ✓✓	5.0177E-15
25-75 h	4.9527E-15	3.21% ($p > 0.2$)	4.7987E-15
75-150 h	4.5985E-15	30.59% ($p = 0.002$ - 0.005)	3.5212E-15

Table 4.16 – *p*-values of the *t-statistics* for Cu-Ni System at 950°C with vs. without Pre-existing Non-uniform Solute Distribution Type B

Ni at%		7.0	11.0	15.0	19.0	23.0	27.0	31.0
0-5 h	p	0.005	0.001	<0.050	0.001	0.001	0.020	0.010
5-25 h	p	0.005	0.010	0.001	>>0.2	0.200	0.020	0.050
25-75 h	p	>>0.2	>>0.2	>>0.2	0.100	>>0.2	>>0.2	>>0.2
75-150 h	p	0.001	0.001	0.002	0.005	0.020	0.020	0.050
Ni at%		35.0 - 95.0						
0-5 h		>>0.050 (No Noticeable Difference)						
5-25 h								
25-75 h								
75-150 h								

4.4.3. Summary of Influence of Pre-existing Non-uniform Solute Distribution

Overall, "**Pre-existing Non-uniform Concentration Solute Distribution Types A and B**" effectively influenced the concentration-dependent interdiffusion coefficient. Therefore, regardless of how the pre-existing non-uniform solute distribution is obtained, it can influence the interdiffusion coefficient in the Cu-Ni system. Due to the previously mentioned strong correlation between DIS and changing $\frac{\partial C}{\partial x}$, the change in the interdiffusion coefficients, which is mainly caused by changing $\frac{\partial C}{\partial x}$ in the Cu-Ni system is attributable to DIS. Accordingly, since $\frac{\partial C}{\partial x}$ also changes with diffusion time, isothermal variation of interdiffusion coefficients with time in the Cu-Ni system is likewise attributable to the DIS.

Additionally, the influence seems to be more significant for shorter diffusion treatments. By comparing the concentration profiles (*Figure 4.16*), it is found that a pre-existing non-uniform solute distribution can undoubtedly cause the variation in $\frac{\partial C}{\partial x}$, but the influence diminishes with diffusion time. The variation is fairly noticeable for 0 h, 5 h, and 25 h of diffusion treatments but negligible for 75 h and 150 h of diffusion treatments. Therefore, this influence might be more profound when the diffusion time is shorter as well, similar to what is mentioned in Section 4.1. Meanwhile, the differences in concentration-dependent interdiffusion coefficients are more evident in the Cu-rich region, similar to the phenomena described in Sections 4.1 and 4.2. Therefore, the time effect might have a more profound effect in the regions that are Cu-rich. To fully confirm that the time effect on interdiffusion coefficients is more profound in the Cu-rich diffusion region and early stage of the interdiffusion, more investigations can be done to obtain a more comprehensive outcome.

5. Summary and Conclusions

The concentration-dependent interdiffusion coefficient has been assumed and generally reported in the literature as an isothermally constant material parameter. The main objective of the present work is to investigate the isothermal time variation of the concentration-dependent interdiffusion coefficient in the Cu-Ni system at elevated temperatures of 900, 950 and 1000°C. In addition, it has been reported in the literature that when DIS is operative during a diffusion process, it can induce the isothermal change of concentration-dependent interdiffusion coefficient when solute concentration gradient ($\frac{\partial C}{\partial x}$) changes.

Therefore, since $\frac{\partial C}{\partial x}$ changes with diffusion time, to investigate whether the isothermal variation of concentration-dependent interdiffusion coefficient with diffusion time in the Cu-Ni system is attributable to DIS, the dependence of the interdiffusion coefficient on $\frac{\partial C}{\partial x}$, when temperature and diffusion time are kept constant is analyzed. This is done by comparing the concentration-dependent interdiffusion coefficient under the condition where uniform or non-uniform solute distribution existed in the material prior to diffusion to when the material was free of pre-existing solute for the same diffusion temperature and time.

The main findings and conclusions are summarised as follows.

1. The concentration-dependent interdiffusion coefficient is observed to isothermally vary with time at the 3 different temperatures, 900, 950 and 1000°C in the Cu-Ni system.
2. At a constant temperature and fixed diffusion time interval, concentration-dependent interdiffusion coefficients when either non-uniform or uniform solute distribution pre-existed

prior to diffusion differ from those of the case where no solute pre-existed in the material prior to the diffusion process.

3. The isothermal variation in the concentration-dependent interdiffusion coefficient at fixed diffusion time intervals due to the presence of either uniform or non-uniform solute distribution is caused by variation in the solute concentration gradients. This strongly indicates that the isothermal variation of the concentration-dependent interdiffusion coefficient in the Cu-Ni system is attributable to DIS, since in the absence of DIS, the concentration-dependent interdiffusion coefficient is independent of the concentration gradient.
4. There are other notable observations in the present work. Isothermal variation of the concentration-dependent interdiffusion coefficient is observed to be more pronounced at the high Cu concentrations and mostly, but not always, occurs during the early diffusion times.
5. Overall, the isothermal time variation of the concentration-dependent interdiffusion coefficient is crucial to the theoretical model prediction and analysis of interdiffusion effects in materials.

6. Limitations and Recommended Future Works

The following are the limitations of this study:

1) The molar volumes (V_m) of Cu and Ni are assumed to be independent on concentration.
2) The 2-profile analytical methods are not accurate at the dilute ends of diffusion couples. Therefore, the $\widetilde{D}(C)$ for 5 at% near both dilute ends are not included.
3) An investigation of impurity diffusion coefficients of Cu and Ni was not included.

The following are some recommendations for future work:

1) Instead of analytical methods, a forward simulation analysis (FSA) can be utilized to obtain interdiffusion and impurity diffusion coefficients in one go.
2) The time effect on activation energy (Q) can be obtained when more temperature conditions and diffusion systems are covered in future works.
3) Investigations of the time effect on interdiffusion coefficients in other binary interdiffusion systems (e.g., Co-Ni) can be done for a more comprehensive result.
4) Apart from single-phase systems (e.g., Cu-Ni system), multiple-phase systems (e.g., Cu-Al system with intermetallic compounds) can be investigated.

References

[1] J. Kučera, K. Cíha, and K. Stránský, “Interdiffusion in the Co-Ni system-I concentration p enetration curves and interdiffusion coefficients,” Czechoslovak Journal of Physics, vol. 2 7, no. 7, pp. 758–768, 1977, doi: 10.1007/BF01589317.

[2] J. HŘebíček, J. Kučera, and K. Stránský, “Determination of interdiffusion coefficients in t he Co-Ni system with the use of spline functions,” Czechoslovak Journal of Physics, vol. 25, no. 10, pp. 1181–1191, 1975, doi: 10.1007/BF01798699.

[3] M. Badia and A. Vignes, “Iron, nickel and cobalt diffusion in transition metals of iron gro up,” Acta Metallurgica, vol. 17, no. 2, pp. 177–187, 1969, doi: 10.1016/0001-6160(69)90 138-2.

[4] G. Opposits, S. Szabó, D. L. Beke, Z. Guba, and I. A. Szabó, “Diffusion-induced bending of Cu-Ni thin sheet diffusion couples,” Scr Mater, vol. 39, no. 7, pp. 977–983, 1998, doi: 10.1016/S1359-6462(98)00228-0.

[5] R. F. Mehl, “Rates of Diffusion in Solid Alloys,” J Appl Phys, vol. 174, no. 8, pp. 174–18 5, 1937, doi: 10.4324/9780203808238-14.

[6] E. O. Kirkendall and A. D. Smigelskas, “Zinc diffusion in alpha brass,” Aime Trans, vol. 171, pp. 130–142, 1947.

[7] G. Grube and R. Haefner, “Die Diffusion der Metalle im festen Zustand,” Zeitschrift für E lektrochemie und angewandte physikalische Chemie, vol. 38, no. 11, pp. 835–842, Nov. 1 932, doi: https://doi.org/10.1002/bbpc.19320381102.

[8] R. F. MEHL and F. N. RHINES, “Rates of diffusion in the alpha solid solutions of copper ,” AIME TRANS, vol. 128, pp. 185–221, 1938.

[9] R. Resnick and R. W. Balluffi, “Diffusion of Zinc and Copper in Alpha and Beta Brasses, ” Jom, vol. 7, no. 9, pp. 1004–1010, 1955, doi: 10.1007/bf03377601.

[10] O. Olaye and O. A. Ojo, “Time variation of concentration-dependent interdiffusion coeffi cient obtained by numerical simulation analysis,” Materialia (Oxf), vol. 16, no. October 2 020, p. 101056, 2021, doi: 10.1016/j.mtla.2021.101056.

[11] D. L. Beke, I. A. Szabó, Z. Erdélyi, and G. Opposits, “Diffusion-induced stresses and thei r relaxation,” Materials Science and Engineering A, vol. 387–389, no. 1-2 SPEC. ISS., pp . 4–10, 2004, doi: 10.1016/j.msea.2004.01.065.

[12] G. B. Stephenson, “Deformation during interdiffusion,” Acta Metallurgica, vol. 36, no. 10 , pp. 2663–2683, 1988, doi: 10.1016/0001-6160(88)90114-9.

[13] Y. Sohn, “Diffusion in metals,” Smithells Metals Reference Book, pp. 1–120, 2003, doi: 10.1016/B978-075067509-3/50016-6.

[14] R. M. White and T. H. Geballe, Diffusion in Solids. 1979.

[15] F. Yang, “Generalized Theory for Diffusion-Induced Stress,” J Electrochem Soc, vol. 168 , no. 4, p. 040520, 2021, doi: 10.1149/1945-7111/abf411.

[16] S. Lou et al., “Insights into interfacial effect and local lithium-ion transport in polycrystall ine cathodes of solid-state batteries,” Nat Commun, vol. 11, no. 1, pp. 1–10, 2020, doi: 10 .1038/s41467-020-19528-9.

[17] Y. Lu and Y. Ni, “Stress-mediated lithiation in nanoscale phase transformation electrodes ,” Acta Mechanica Solida Sinica, vol. 30, no. 3, pp. 248–253, 2017, doi: 10.1016/j.camss. 2017.05.004.

[18] H. K. D. H. Bhadeshia, “A commentary on: ‘Diffusion of carbon in austenite with a disco ntinuity in composition,’” Metall Mater Trans A Phys Metall Mater Sci, vol. 41, no. 7, pp . 1605–1615, 2010, doi: 10.1007/s11661-010-0276-5.

[19] P. Dłuzewski, “Nonlinear field theory of the stress induced interdiffusion and mass transp ort,” Defect and Diffusion Forum, vol. 264, pp. 63–70, 2007, doi: 10.4028/3-908451-41-8 .63.

[20] Y. Chen, Z. Li, L. Qi, Y. Zhang, and C. Chen, “Diffusion-induced Stresses in Solids,” Ac ta Materialia Sinica, vol. 42, no. 3, pp. 225–233, 2006, doi: 10.3321/j.issn:0412-1961.200 6.03.001.

[21] N. Itoh and T. Nakau, “Penetration depth of diffusion-induced dislocations,” Jpn J Appl P hys, vol. 22, no. 7R, pp. 1106–1111, 1983, doi: 10.1143/JJAP.22.1106.

[22] I. Daruka, I. A. Szabó, D. L. Beke, C. Cserháti, A. Kodentsov, and F. J. J. van Loo, “Diffu sion-induced bending of thin sheet couples: Theory and experiments in Ti-Zr system,” Ac ta Mater, vol. 44, no. 12, pp. 4981–4993, 1996, doi: 10.1016/S1359-6454(96)00099-7.

[23] D. W. Stevens and G. W. Powell, “Diffusion-Induced Stresses and Plastic Deformation.,” Metall Trans A, vol. 8 A, no. 10, pp. 1531–1541, 1977, doi: 10.1007/BF02644856.

[24] D. L. Beke, Z. Erdélyi, and B. Parditka, “Effect of diffusion induced driving forces on int erdiffusion - Stress development/relaxation and kinetics of diffusion processes,” Defect a nd Diffusion Forum, vol. 309–310, pp. 113–120, 2011, doi: 10.4028/www.scientific.net/D DF.309-310.113.

[25] O. Olaye, “NUMERICAL ANALYSIS OF ISOTHERMAL VARIATION OF CONCEN TRATION-DEPENDENT INTERDIFFUSION COEFFICIENT,” 2022.

[26] L. A. Girifalco and H. H. Grimes, “Effect of Static Strains on Diffusion,” 1961.

[27] J. L. Chu and S. Lee, “The effect of chemical stresses on diffusion,” J Appl Phys, vol. 75, no. 6, pp. 2823–2829, 1994, doi: 10.1063/1.356174.

[28] R. K. Jain and R. J. van Overstraeten, “Calculation of the diffusion induced stresses in sili con,” physica status solidi (a), vol. 25, no. 1, pp. 125–130, 1974, doi: 10.1002/pssa.22102 50109.

[29] Z. Wang, L. Fang, I. Cotton, and R. Freer, “Ni-Cu interdiffusion and its implication for ag eing in Ni-coated Cu conductors,” Mater Sci Eng B Solid State Mater Adv Technol, vol. 1 98, pp. 86–94, 2015, doi: 10.1016/j.mseb.2015.04.006.

[30] Q. Zhang, Z. Chen, W. Zhong, and J. C. Zhao, “Accurate and efficient measurement of im purity (dilute) diffusion coefficients without isotope tracer experiments,” Scr Mater, vol. 128, pp. 32–35, 2017, doi: 10.1016/j.scriptamat.2016.09.040.

[31] A. Borgenstam, A. Engstro, L. Ho Lund, and J. A. Ren, “Basic and Applied Research: Se ction I DICTRA, a Tool for Simulation of Diffusional Transformations in Alloys,” Journa l of phase equilibria, vol. 21, no. 3, pp. 269–280, 2000.

[32] Q. Zhang and J. C. Zhao, “Extracting interdiffusion coefficients from binary diffusion cou ples using traditional methods and a forward-simulation method,” Intermetallics (Barking), vol. 34, pp. 132–141, 2013, doi: 10.1016/j.intermet.2012.11.012.

[33] L. Kaufman and J. Ågren, “CALPHAD, first and second generation - Birth of the materia ls genome,” Scr Mater, vol. 70, no. 1, pp. 3–6, 2014, doi: 10.1016/j.scriptamat.2012.12.00 3.

[34] Z. Chen, Q. Zhang, and J. C. Zhao, “Pydiffusion: A Python library for diffusion simulatio n and data analysis,” J Open Res Softw, vol. 7, no. 1, pp. 1–7, 2019, doi: 10.5334/jors.255 .

[35] Mathworks, “Piecewise Cubic Hermite Interpolating Polynomial (PCHIP) MATLAB Onl ine Help Centre,” 2022. https://www.mathworks.com/help/matlab/ref/pchip.html

[36] Q. Zhang and J. C. Zhao, “Impurity and interdiffusion coefficients of the Cr-X (X = Co, F e, Mo, Nb, Ni, Pd, Pt, Ta) binary systems,” J Alloys Compd, vol. 604, pp. 142–150, 2014, doi: 10.1016/j.jallcom.2014.03.092.

[37] R. Kulik and P. Soulier, “Moving averages,” Springer Series in Operations Research and Financial Engineering, pp. 425–452, 2020, doi: 10.1007/978-1-0716-0737-4_15.

[38] O. Olaye and O. A. Ojo, “A New Analytical Method for Computing Concentration-Depen dent Interdiffusion Coefficient in Binary Systems with Pre-existing Solute Concentration

Gradient," J Phase Equilibria Diffus, vol. 42, no. 2, pp. 303–314, 2021, doi: 10.1007/s11669-021-00883-z.

[39] M. Tanner, H. P. Beck, I. Felger, and T. Smith, Diffusion in Solid Metals and Alloys. 1990. doi: 10.1016/S0035-9203(99)90319-X.

[40] A. P. Varun A. Baheti, "Development of different methods and their efficiencies for the estimation of diffusion coefficients following the diffusion couple technique," Acta Mater, vol. 156, no. August, p. 2018, 2018.

[41] S. M. Schwarz, B. W. Kempshall, and L. A. Giannuzzi, "Effects of diffusion induced recrystallization on volume diffusion in the copper-nickel system," Acta Mater, vol. 51, no. 10, pp. 2765–2776, 2003, doi: 10.1016/S1359-6454(03)00082-X.

[42] T. Lin et al., "An investigation on diffusion bonding of Cu/Cu using various grain size of Ni interlayers at low temperature," Materialia (Oxf), vol. 14, no. May, p. 100882, 2020, doi: 10.1016/j.mtla.2020.100882.

[43] H. Mehrer and S. Divinski, "Diffusion in metallic elements and intermetallics," Defect and Diffusion Forum, vol. 289–292, no. April 2009, pp. 15–38, 2009, doi: 10.4028/www.scientific.net/DDF.289-292.15.

[44] V. Rothová, M. Svoboda, and J. Buršík, "The effect of annealing conditions on grain growth and microstructure in nickel," METAL 2009 - 18th International Conference on Metallurgy and Materials, Conference Proceedings, no. October 2015, pp. 473–480, 2009.

[45] S. Prussin, "Generation and distribution of dislocations by solute diffusion," J Appl Phys, vol. 32, no. 10, pp. 1876–1881, 1961, doi: 10.1063/1.1728256.

[46] G. Britain and H. Francombe, "Measurement of Diffusion-induced Strains at Metal Bond Interfaces," Solid State Electron, vol. 11, pp. 205–208, 1968.

[47] B. Wu, B. Chen, Z. Zou, S. Liao, and W. Deng, "Thermal stability of ultrafine grained pure copper prepared by large strain extrusion machining," Metals (Basel), vol. 8, no. 6, pp. 1–13, 2018, doi: 10.3390/met8060381.

[48] B. Tas Kavakbasi, I. S. Golovin, A. Paul, and S. v. Divinski, "On the analysis of composition profiles in binary single-phase diffusion couples: Systems with a strong compositional dependence of the interdiffusion coefficient," Defect and Diffusion Forum, vol. 383, pp. 23–30, 2018, doi: 10.4028/www.scientific.net/DDF.383.23.